

Sources of Beam Instability

- **Magnetic Field Errors**

- **Mechanical**

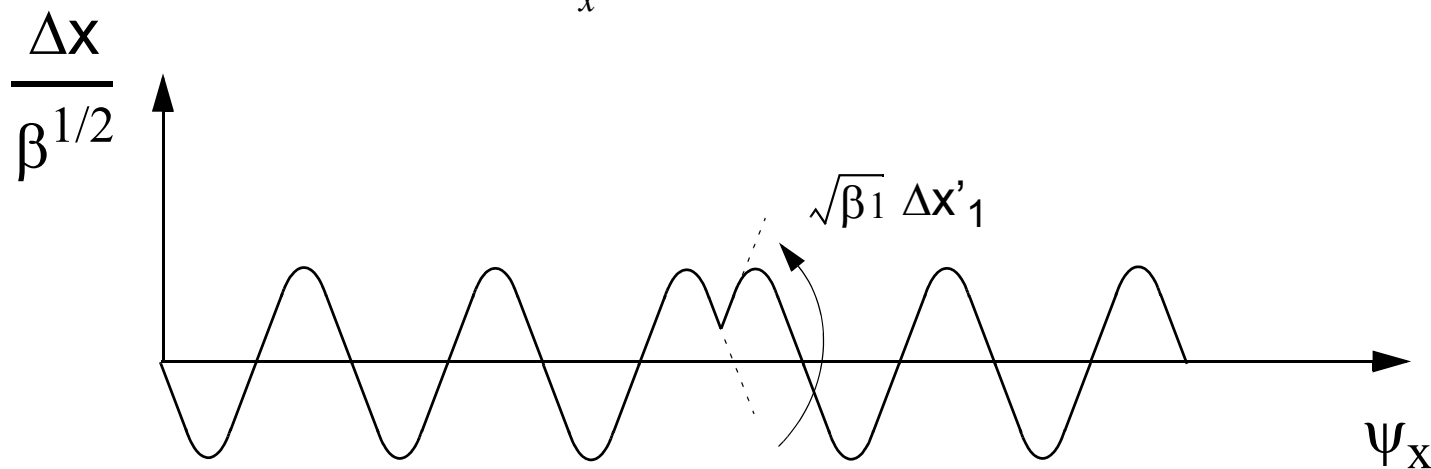
Sources of Beam Instability - Magnetic Field Errors

A localized change in transverse magnetic field $\delta B(s)$ will introduce a kick

$$\Delta x' = \frac{1}{B\rho} \int \delta B(s) ds$$

which in turn will cause a closed orbit distortion with a kink in it:

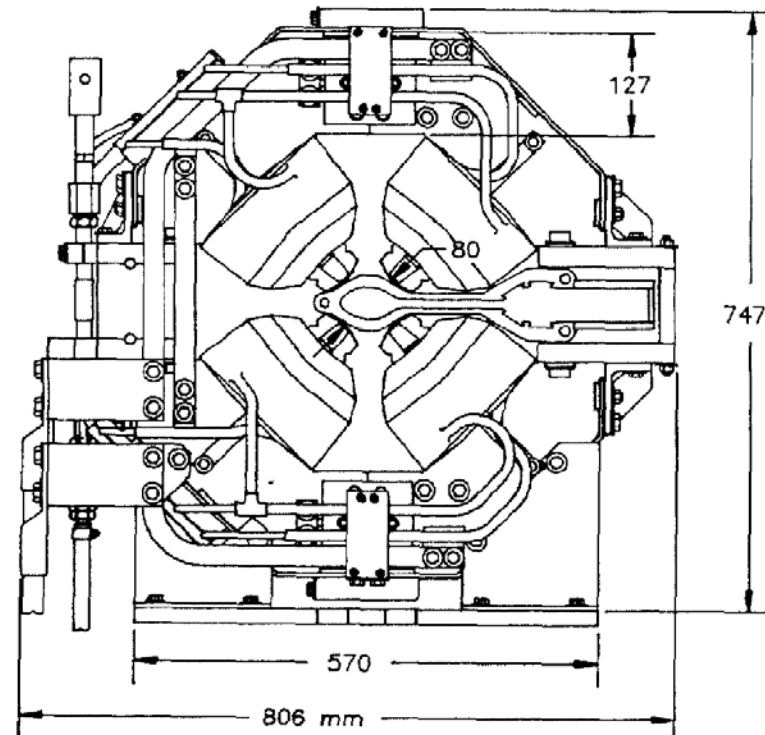
$$\begin{aligned} \Delta x(s) &= \frac{\sqrt{\beta_x(s)\beta_1} \Delta x_1'}{2 \sin \pi \nu_x} \cos[\psi_x(s) - \psi_x(s_1) + \nu_x \pi] \quad s < s_1 \\ &= \frac{\sqrt{\beta_x(s)\beta_1} \Delta x_1'}{2 \sin \pi \nu_x} \cos[\psi_x(s_1) - \psi_x(s) + \nu_x \pi] \quad s > s_1 \end{aligned}$$



Sources of Beam Instability - Quadrupole Magnetic Field Errors

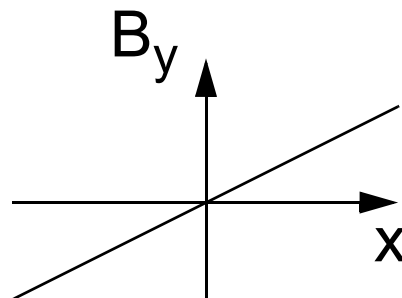
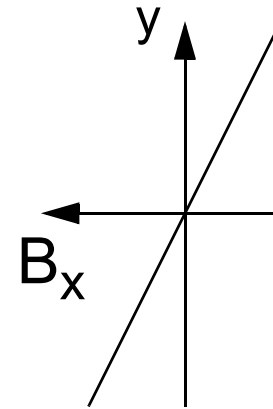
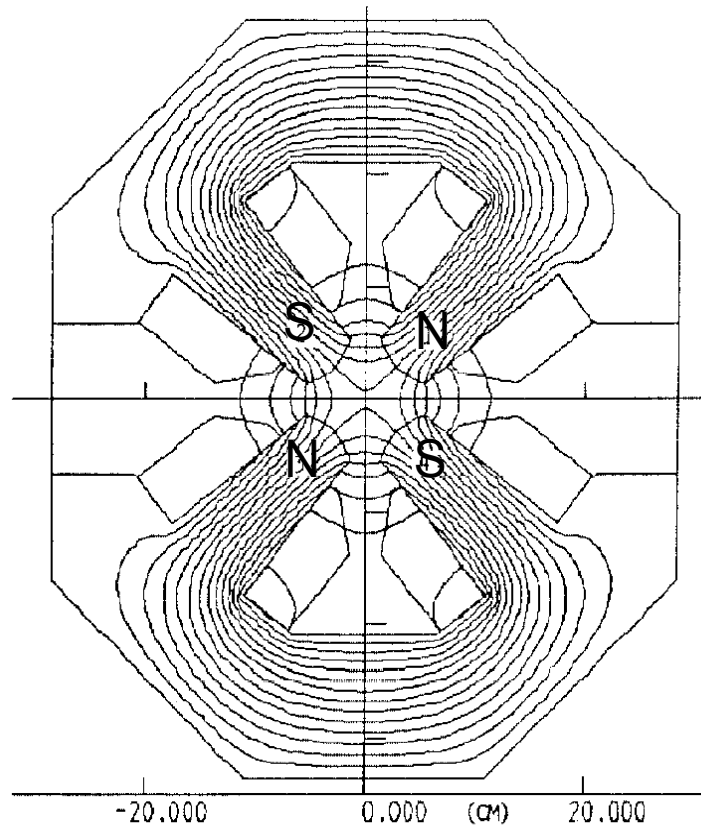
Table 1 - Quadrupole Parameters

Strength	20 T/m	←
Bore Diameter	80 mm	
Effective Length	0.8 m	←
Turns/pole	33	
Conductor Height	11.5 mm	
Width	11.5 mm	
Hole Diameter	6.3 mm	
Inductance	29 mH	
Resistance	45 mΩ	
Current	414 A	
Current Density in Coil	2.5 A/mm ²	
Voltage	19 V	
Power	7.9 kW	
Water Flow	2.7 gal/min	
Water Pressure Drop	40 psi	
Water Temperature Rise	11 °C	

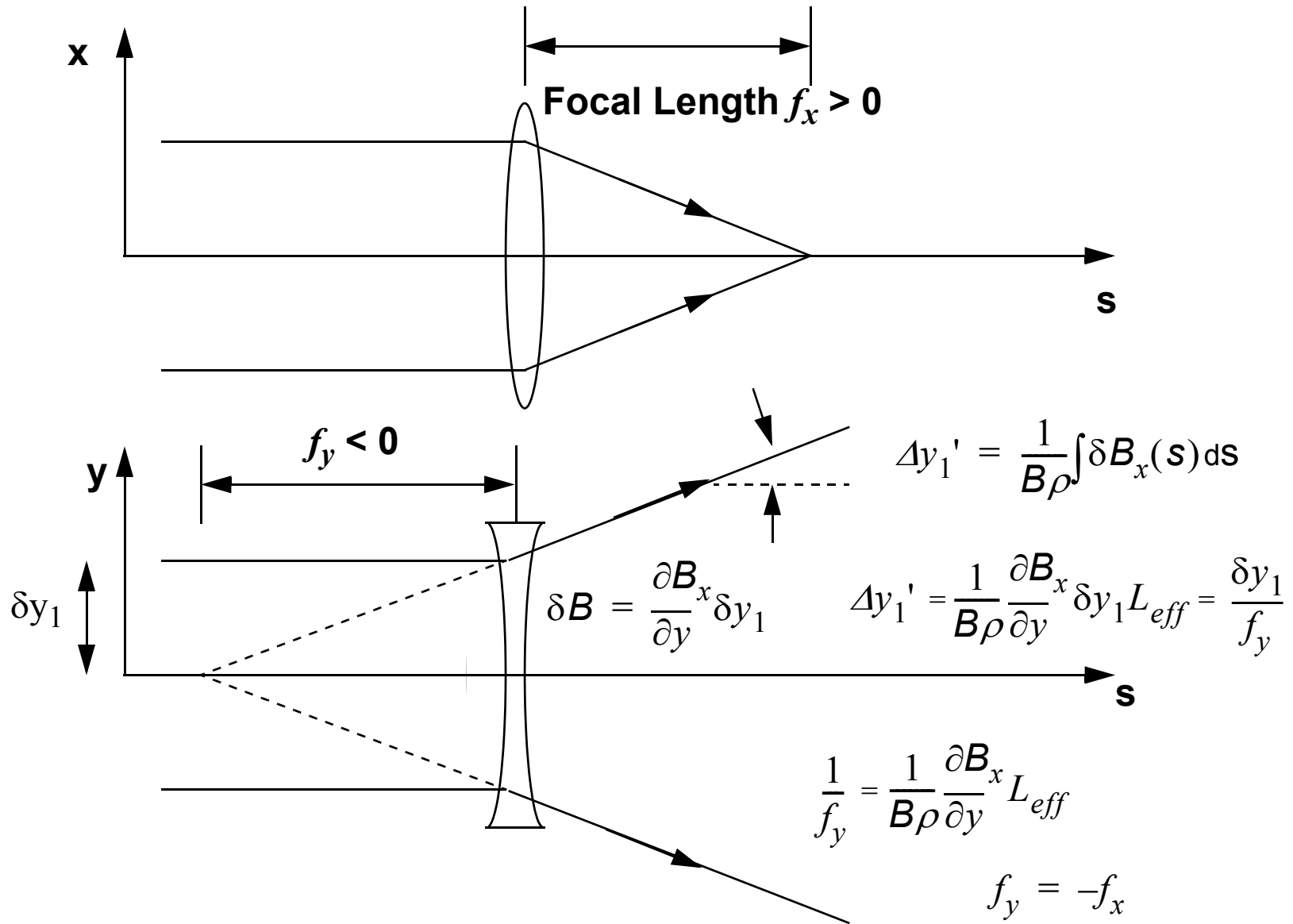


K. Thompson et al, http://accelconf.web.cern.ch/accelconf/p89/PDF/PAC1989_0396.PDF

Quadrupole Magnetic Field



Quadrupole Magnetic Focussing Properties



Quadrupole Misalignment Amplification Factor

Closed orbit distortion $\Delta y(s)$ resulting from the misalignment of a quadrupole with focal length f_y by an amount δy_1

$$\Delta y(s) = \frac{\sqrt{\beta_x(s)\beta_1} \Delta y_1'}{2 \sin \pi \nu_y} \cos[\psi_y(s) - \psi_y(s_1) + \nu_x \pi] \quad \Delta y_1' = \frac{\delta y_1}{f_y}$$

The cumulative effect of the uncorrelated misalignment of N quadrupole magnets is to produce an rms closed orbit deviation

$$\sigma_{co}(s) = \frac{\sqrt{\beta_x(s)\langle\beta\rangle} \sigma_q}{2 \sin \pi \nu_x |f_x| \sqrt{2}} \leftarrow$$

where σ_q is the rms amount of quadrupole misalignment. This formula was derived for a simple FODO lattice, where focussing and defocussing quads have the same focal length, but with opposite sign, although the general behaviour is similar for any storage ring.. The quantity $\langle\beta\rangle$ is the average beta function at the quadrupole locations.

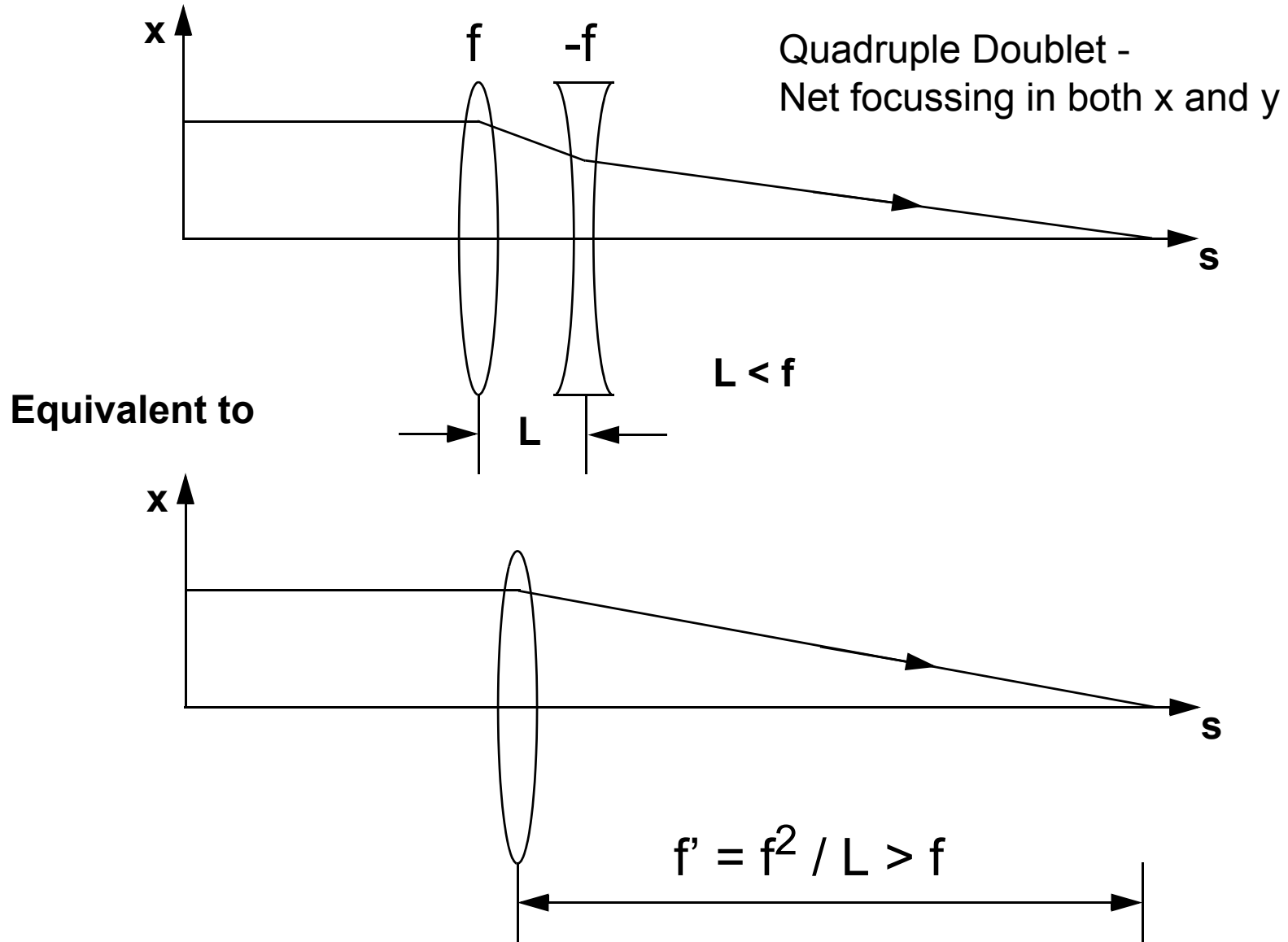
J. Rossbach, Particle Accelerators, 1998, Vol. 23, pp.121-132

Ramifications of Amplification Factor for Orbit Stabilization

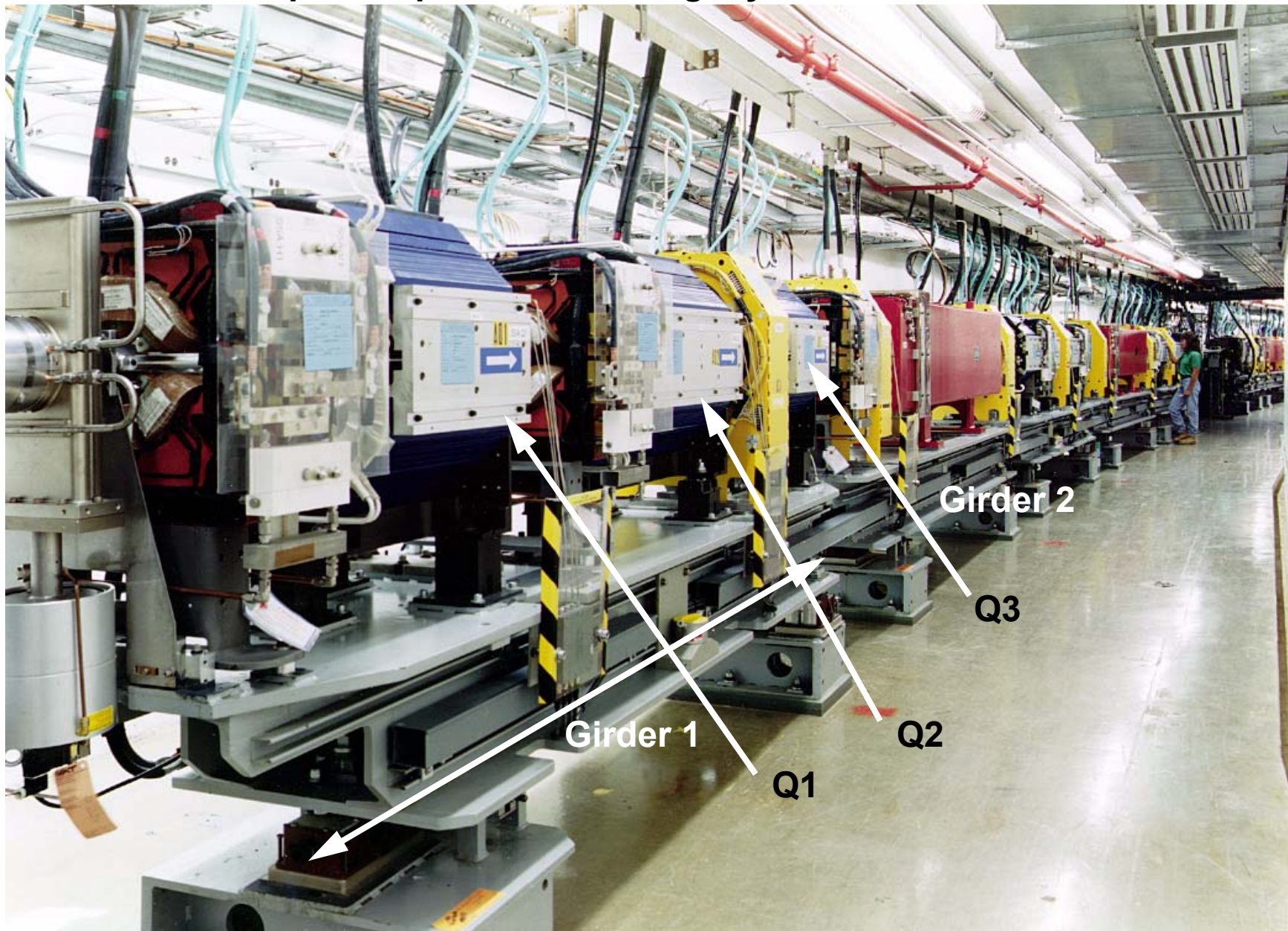
$$\sigma_{co}(s) = \frac{\sqrt{\beta_x(s)\langle\beta\rangle}}{2 \sin \pi \nu_x} \frac{\sigma_q}{|f|} \sqrt{\frac{N}{2}}$$

- 1) Formula is valid for time-dependent quadrupole misalignment, i.e. vibrations
- 2) Machines with strong focussing (small f --> large field gradient) are potentially very susceptible to large amplification of tiny magnet motions. All modern light sources have extremely strong focussing.
- 3) It gets worse for larger machines as the square root of N . For APS, $N = 400$

Design Trick to Fool the Machine



Quadrupole Triplet Mounted Rigidly on a Common Girder



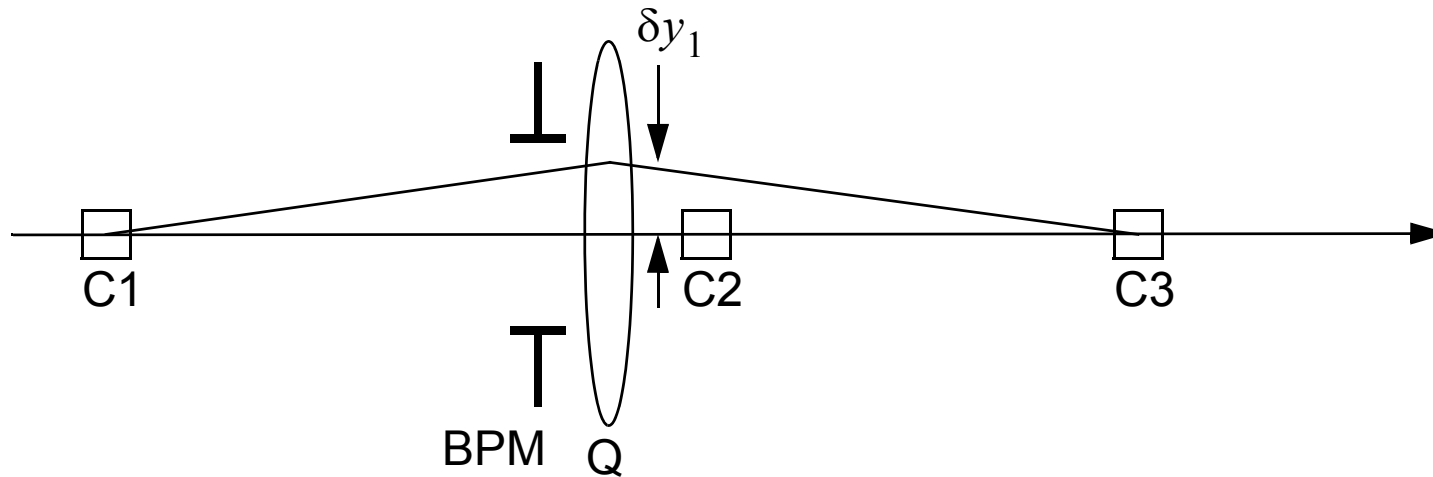
Amplification Factor for Rigidly Mounted Quad Multiplets

$$\sigma_{co}(s) = \frac{\sqrt{\beta_x(s) \langle \beta \rangle}}{2 \sin \pi \nu_x} \frac{\sigma_q}{\sqrt{2}} \sqrt{N}$$

Now $N = 120$ Girders vs. 400 Quadrupoles, $f_{\text{triplet}} > f_{\text{quad}}$, $\sigma_q \rightarrow \sigma_g$, the rms girder displacement. At the APS, the amplification assuming uncorrelated quadrupole motion was approx. 50 vs. 20 when grouped by girder.

Application of Quadrupole Displacement Formula to Beam-Based Alignment

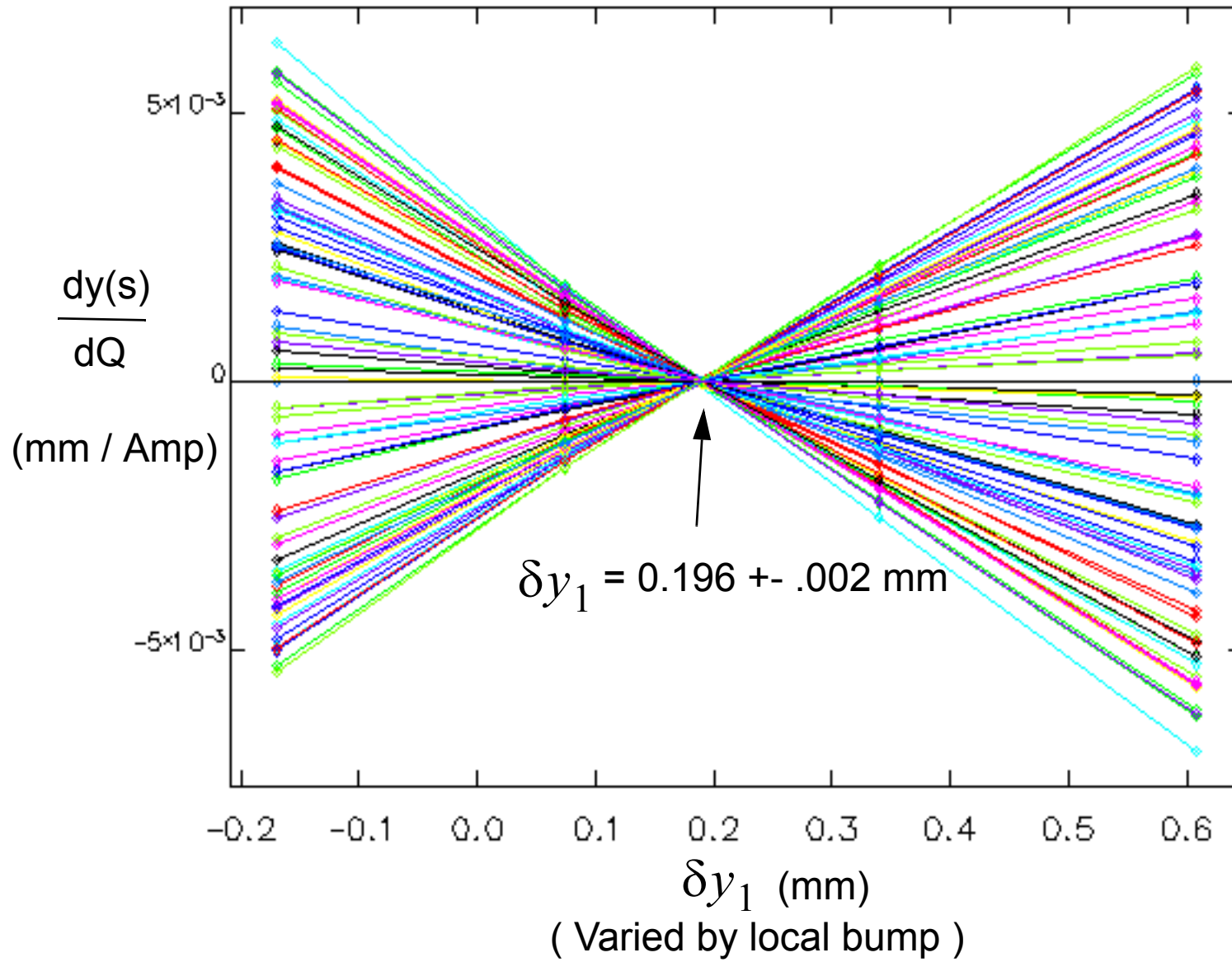
$$\Delta y(s) = \frac{\sqrt{\beta_x(s)\beta_1} \Delta y_1'}{2 \sin \pi \nu_y} \cos[\psi_y(s) - \psi_y(s_1) + \nu_x \pi] \quad \Delta y_1' = \frac{\delta y_1}{f_y}$$



Correctors C1, C2, C3 form a closed bump to vary δy_1

Unless $\delta y_1 = 0$, a small change in the strength of Q will cause a global orbit distortion according to the above formula

Experimental Determination of BPM - Quad Offset



Geophysics

Equation of Motion, Homogenous, Isotropic Media

$$\rho \frac{\partial^2 u_i}{\partial t^2} - (\kappa + \mu) \frac{\partial^2 u_j}{\partial x_i \partial x_j} - \mu \frac{\partial^2 u_i}{\partial x_j^2} = f_i.$$

Ansatz u_i = displacement vector field

$$\vec{u} = \nabla \phi + \nabla \times \vec{\psi} = \text{grad } \phi + \text{curl } \vec{\psi},$$

Compressional P-waves

$$\frac{\partial^2 \phi}{\partial t^2} = c^2 \nabla^2 \phi,$$

Shear S-waves

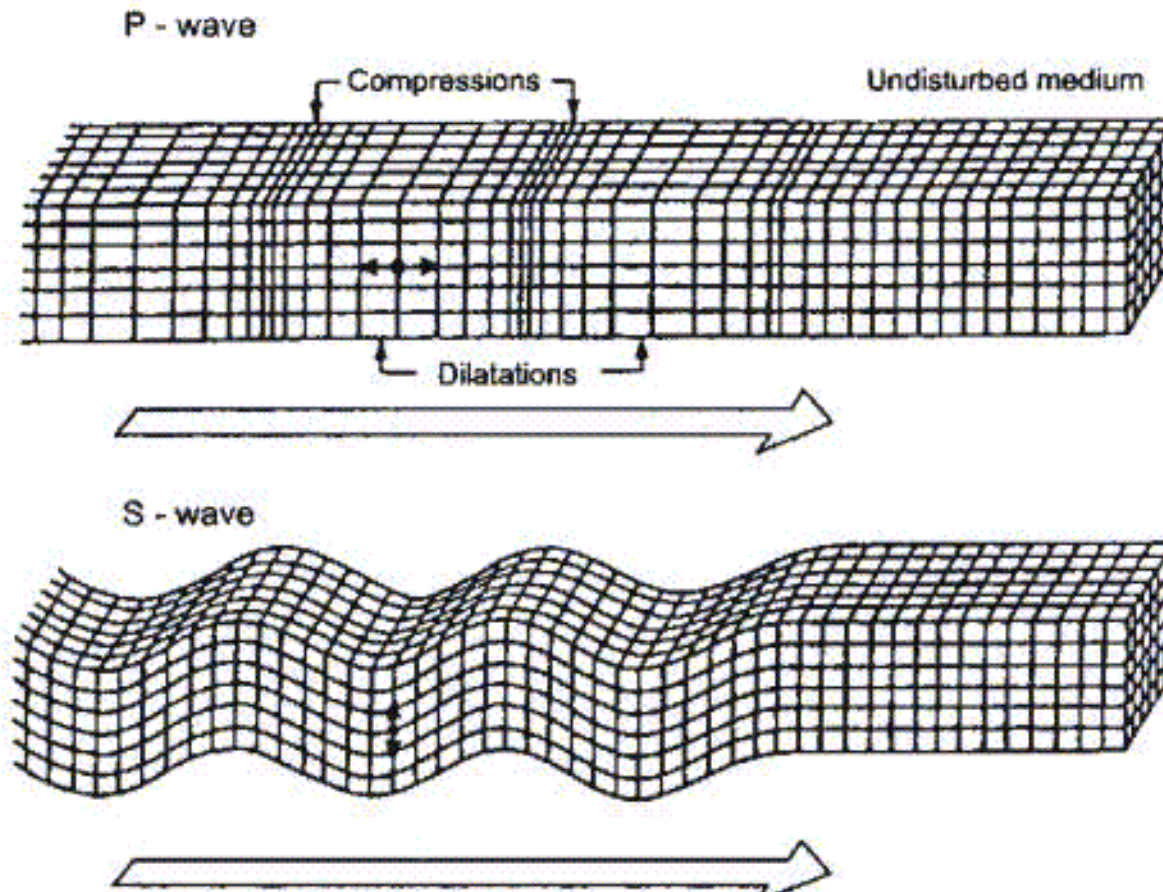
$$\frac{\partial^2 \vec{\psi}}{\partial t^2} = b^2 \nabla^2 \vec{\psi},$$

$c = \sqrt{(\kappa + \frac{4}{3}\mu)/\rho}$ is the P-wave velocity, $b = \sqrt{\mu/\rho}$ is the S-wave velocity.

ρ = mass density - kg / m³
 μ = shear modulus of elasticity
 κ = bulk modulus

Ilya Tsvankin, "Seismic Wavefields in Layered Isotropic Media"
Colorado School of Mines Geophysics Dept.

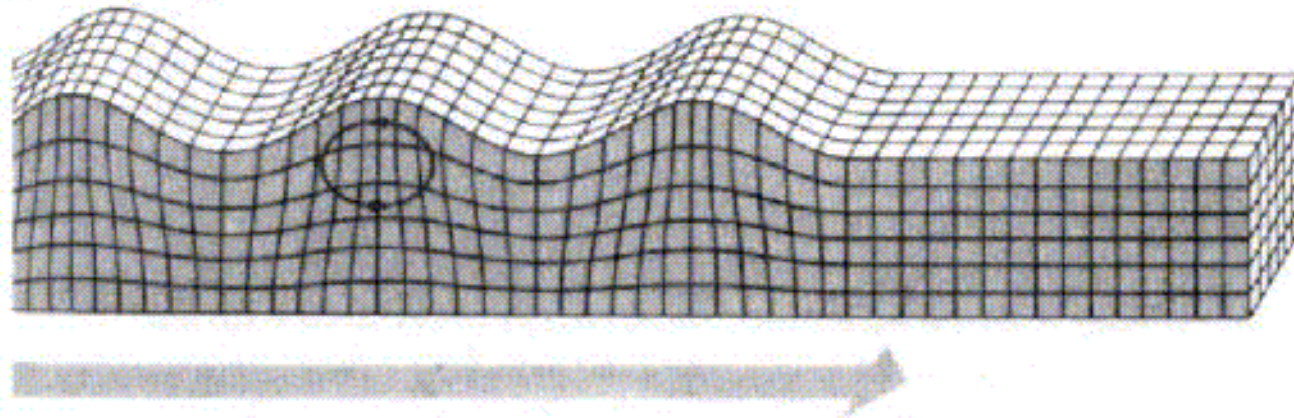
Geometry Associated with Compressional (P) and Shear (S) Waves (Body Waves)



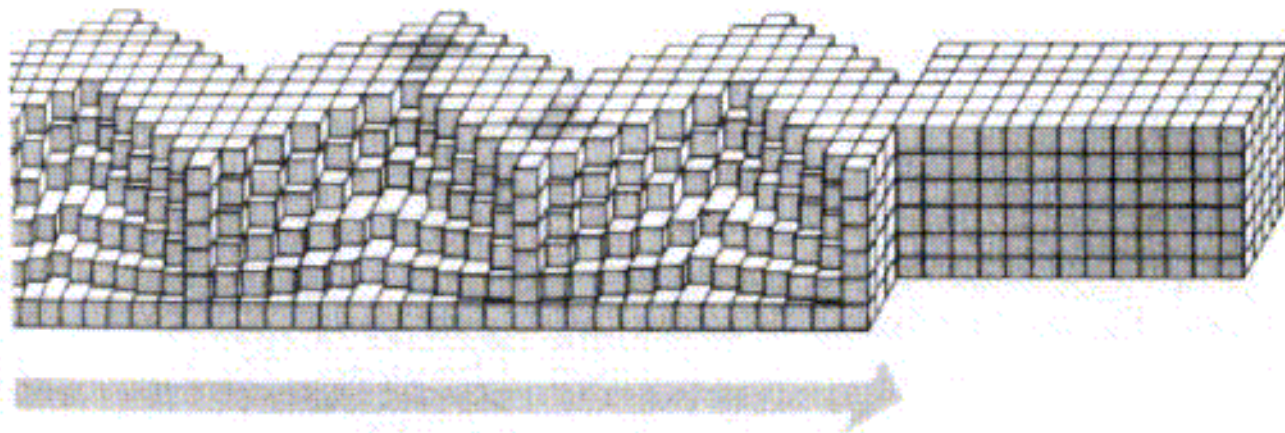
http://www.sfu.ca/earth-sciences/courses/317Spring02/4-Earthquake_Seismology.htm

Yet More Flavors of Seismic Vibrations (Surface Waves)

(a) Rayleigh wave



(b) Love wave



http://www.sfu.ca/earth-sciences/courses/317Spring02/4-Earthquake_Seismology.htm

Material Properties and Seismic Wave Velocities for Various Rock Types

Material	P-wave Velocity C_p (km/s)	S-wave Velocity C_s (km/s)	Bulk Modulus K (GPa)	Rigidity Modulus μ (GPa)	Density ρ (kg/m ³)	Poisson's Ratio σ	Young's Modulus Y (GPa)
Granite	5.5	3.0	49	24	2700	0.29	13.8
Shale	2.2	0.81	9.91	1.64	2500	0.42	1.0
Limestone	6	3	65	24	2700	0.33	14.4
Austin Chalk	2.530	1.219	9.55	3.21	2160	0.35	1.9
Bunter Sandstone	0.76	0.44	0.67	0.40	2080	0.25	1.0

D. Holder, CLRC Daresbury Report AP-BU-rpt-001

<http://www.astec.ac.uk/diamond/notes/ap/AP-BU-rpt-001-Ground%20Motion%20Intro.doc>

Frequency Scales Associated with Ground Vibration

Machine	Diameter	Revolution Frequency	Frequency at which $\lambda = D$, @v=750 m/s
SPEAR	74.6 meters	1.3 MHz	10 Hz
PEP	700 meters	136 kHz	1 Hz
Tevatron	2 km	47 kHz	0.3 Hz

G. Fischer, AIP153, pp. 1047-1119

Accelerator / Ground Motion Resonance Condition

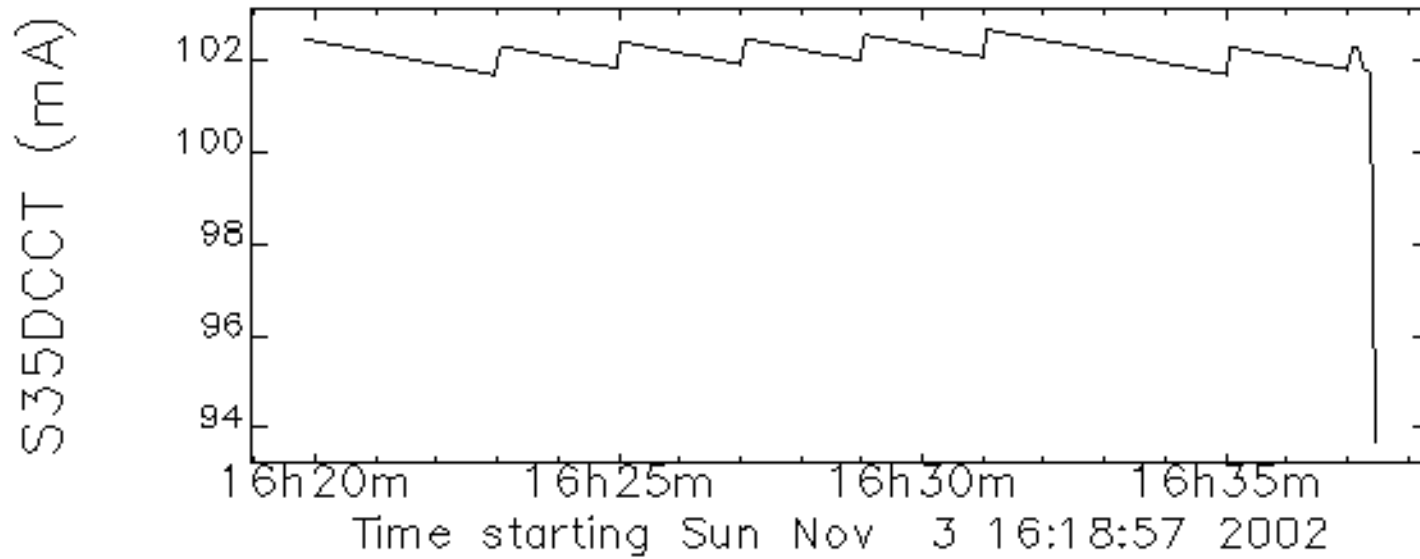
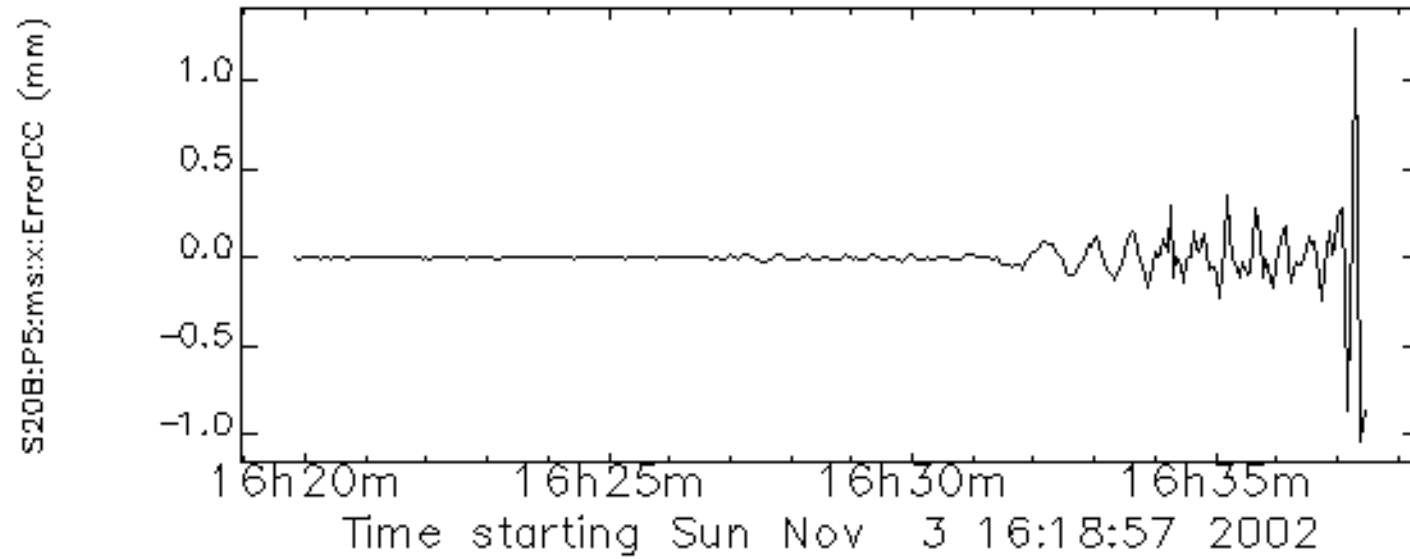
When the wavelength of seismic waves approaches the ring dimensions, an amplification effect takes place whereby the amplitude of closed orbit distortion can be many times larger than the amplitude of ground motion. This resonance condition occurs when

$$\frac{C}{\lambda} = \nu, N - \nu, N + \nu$$

where C is the ring circumference, N is the number of superperiods, and ν is the fractional part of the tune (vertical or horizontal).

J. Rossbach, Particle Accelerators, 1998, Vol. 23, pp.121-132

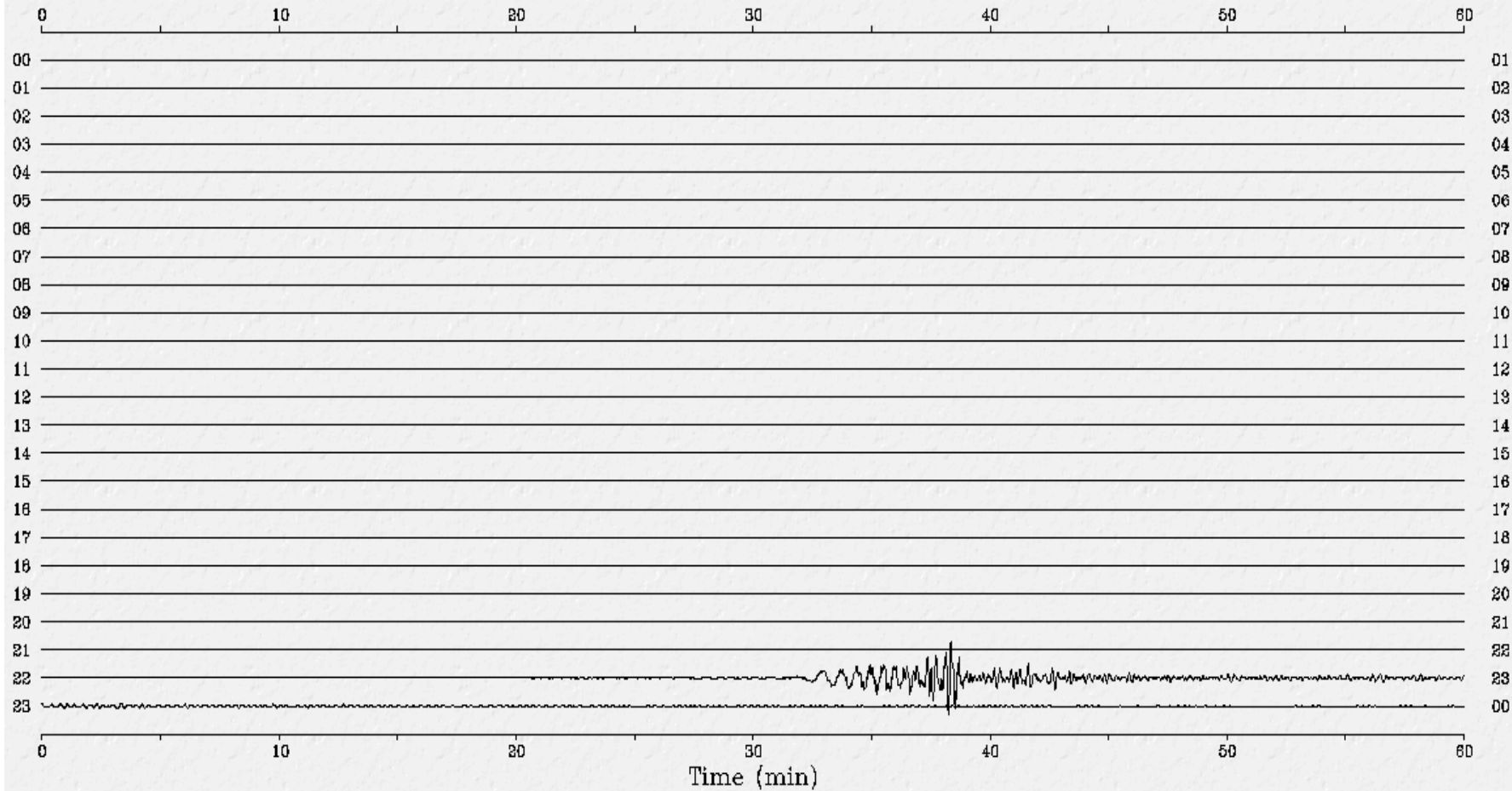
Response of Horizontal Beam Position to an Earthquake in Alaska



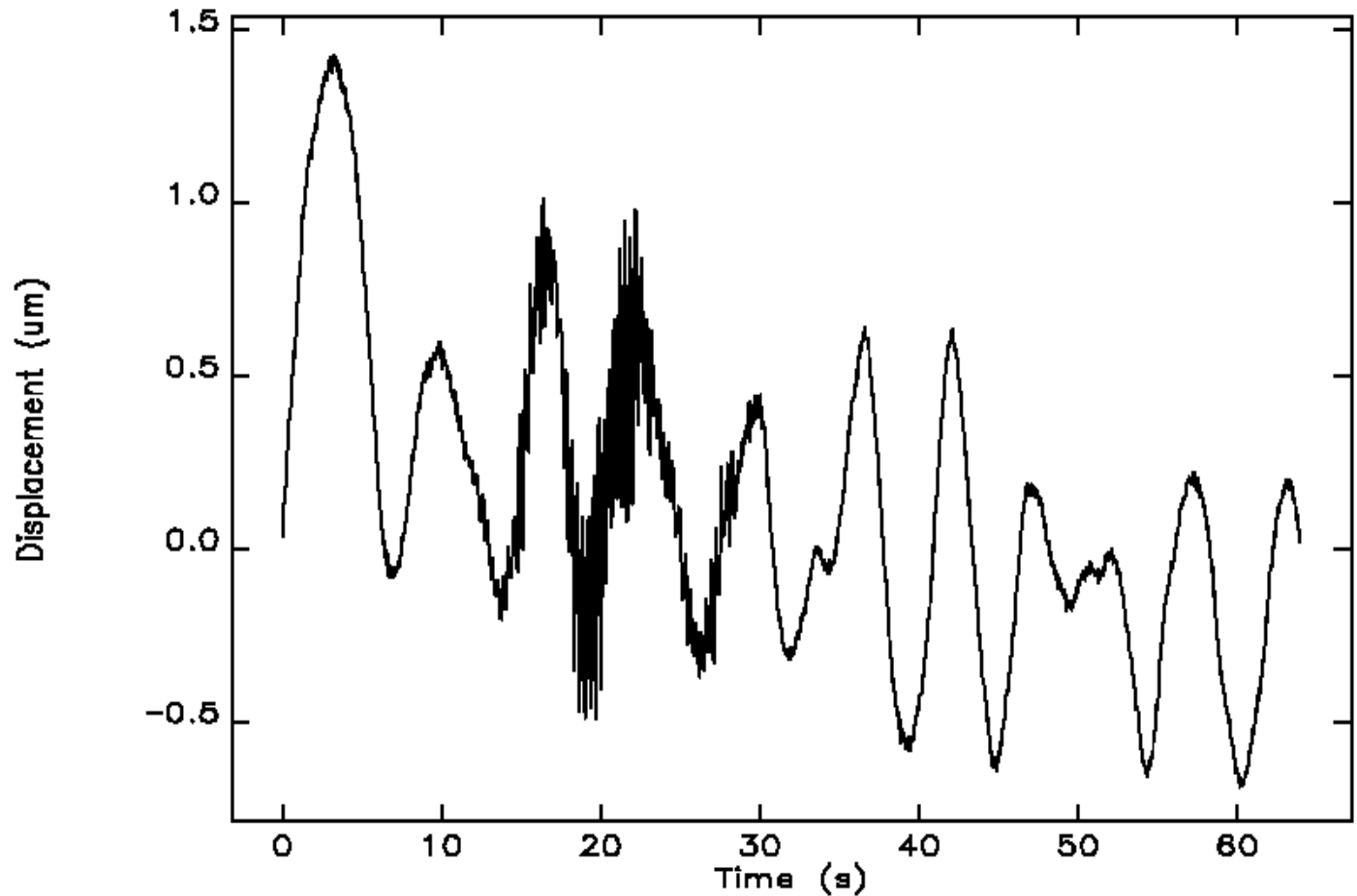
Seismogram of Alaskan Earthquake 11/3/02

Seismogram for AAM
Ann Arbor, Michigan, USA

Station: AAM LHZ
2002 NOV 3 UTC
Start: 00:00:00.21

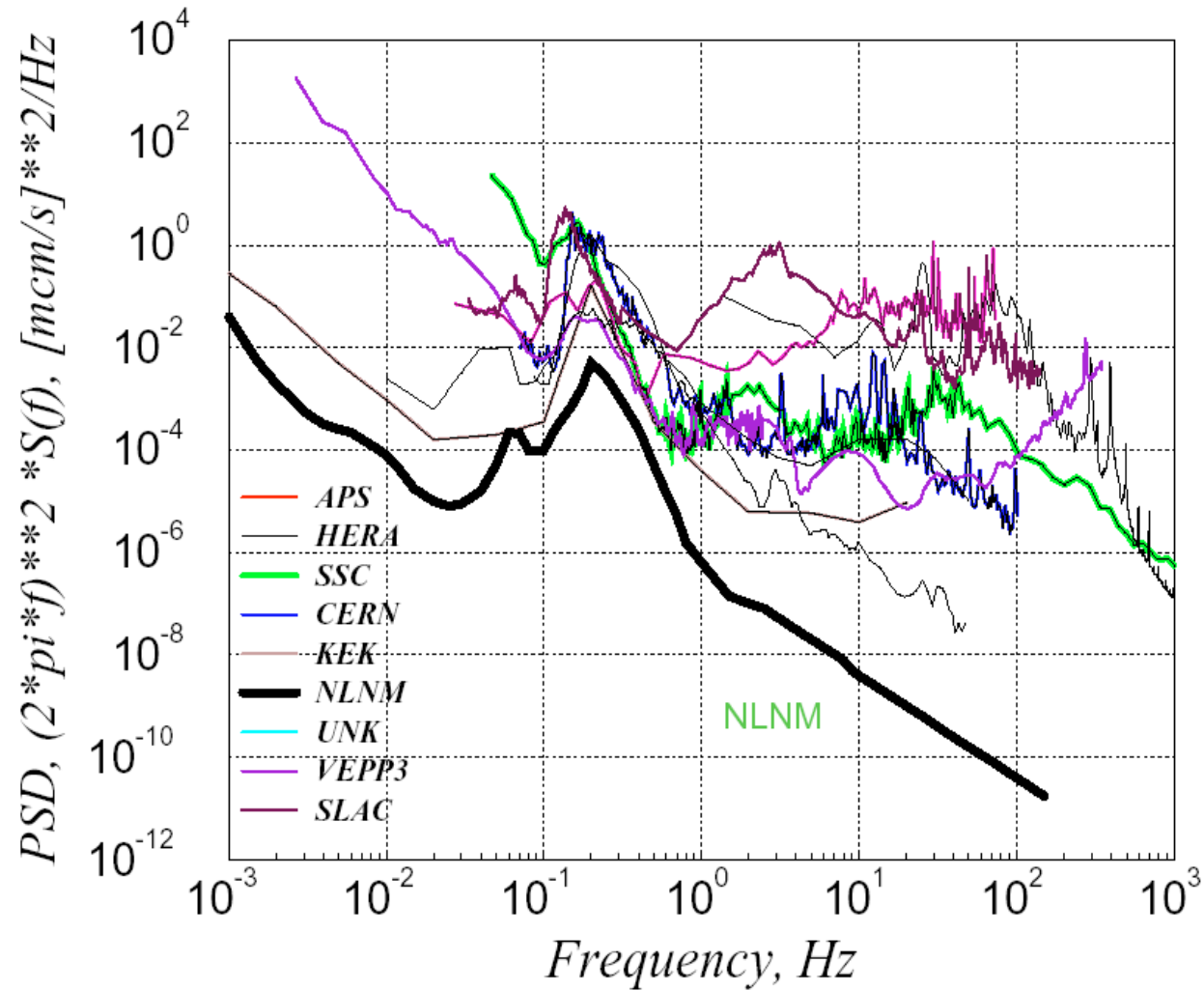


Ground Motion at APS Sector 19 resulting from Driving a Fork Truck Under the Ring



Time Record: Vertical Motion While 23000 lb forklift Passes Through Vehicle Tunnel

Velocity Power Spectral Density Around the World



V. Shiltsev, <http://epaper.kek.jp/e96/PAPERS/ORALS/TUY03A.PDF>

Space-Time Ground Diffusion (The ATL Law)

The mean square relative displacement (variance) of two points a distance L apart grows linearly with time T according to

$$\langle dX^2 \rangle = ATL$$

where A is on the order of $10^{-5 \pm 1} \mu\text{m}^2 / \text{sec} / \text{meter}$.

This results in power spectral densities in time and space as follows:

$$S_{ATL}(\omega) = \frac{2AL}{\omega^2} ; \quad \omega = 2\pi f > 0 \quad S_{ATL}(k) = \frac{2AT}{k^2} ; \quad k = \frac{2\pi}{\lambda} > 0$$

V. Shiltsev, 1995 Workshop on Accelerator Alignment
http://www.slac.stanford.edu/grp/met/TOC_S/1995conf.htm
http://www.slac.stanford.edu/grp/met/TOC_S/Papers/VShil95.pdf

PSD of Closed Orbit Distortion at HERA, Using $\beta = 1$ meter

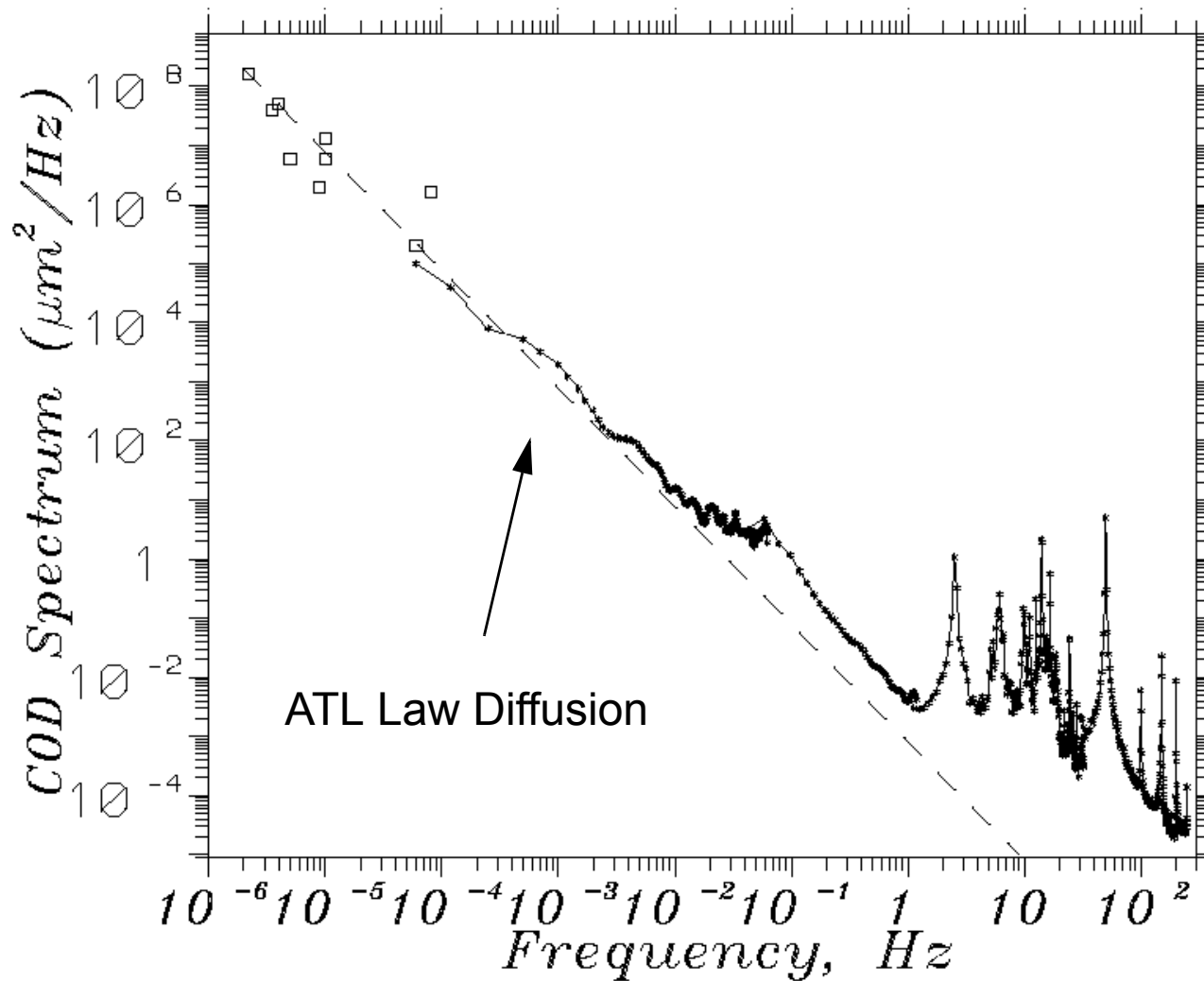
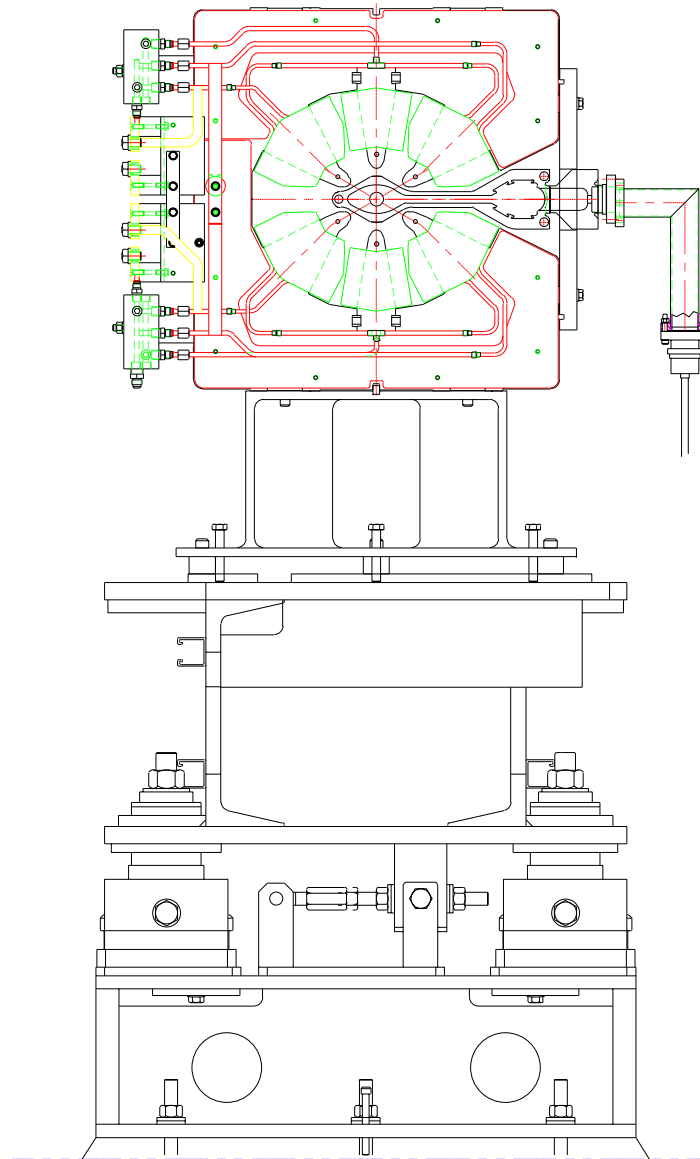


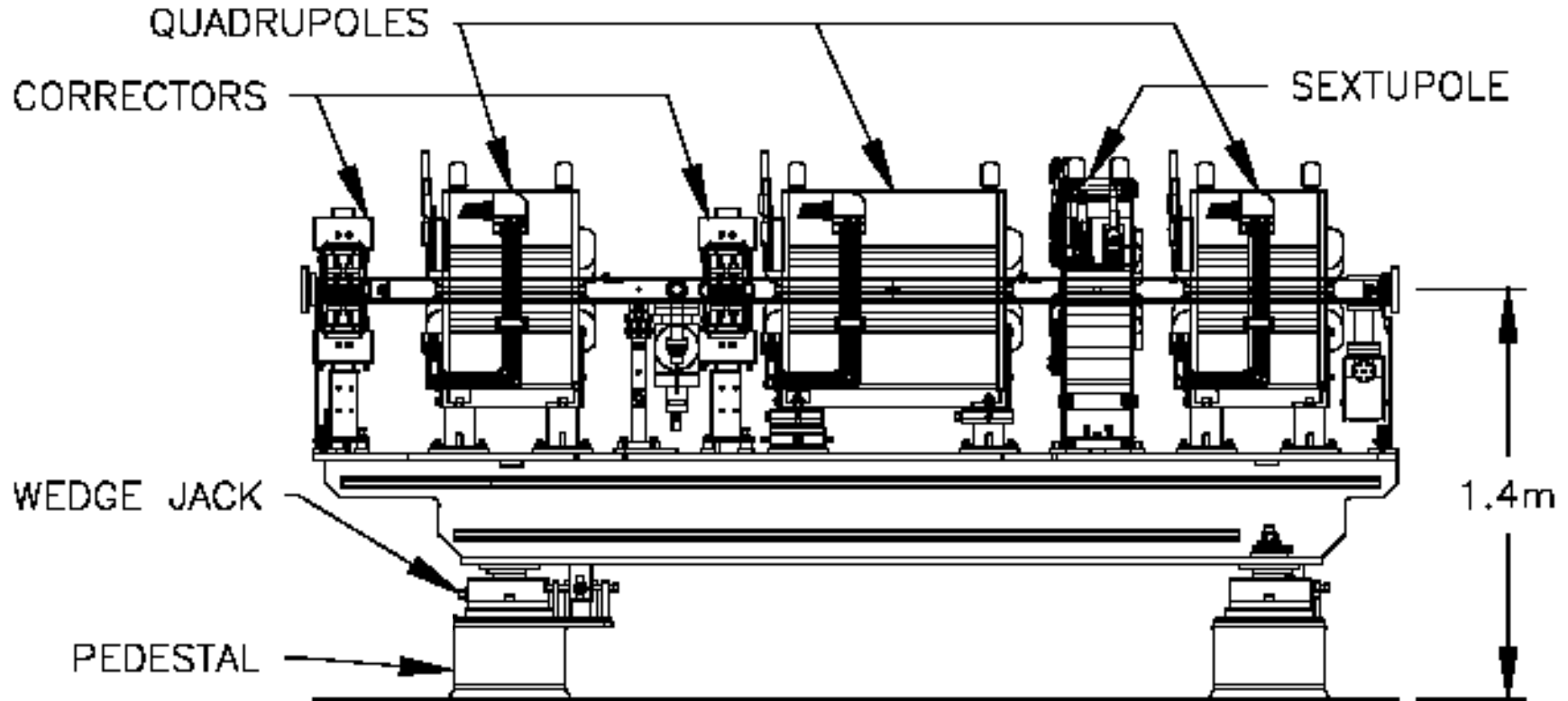
Figure 5: Spectrum of vertical COD at HERA-p.

V. Shiltsev, <http://epaper.kek.jp/e96/PAPERS/ORALS/TUY03A.PDF>

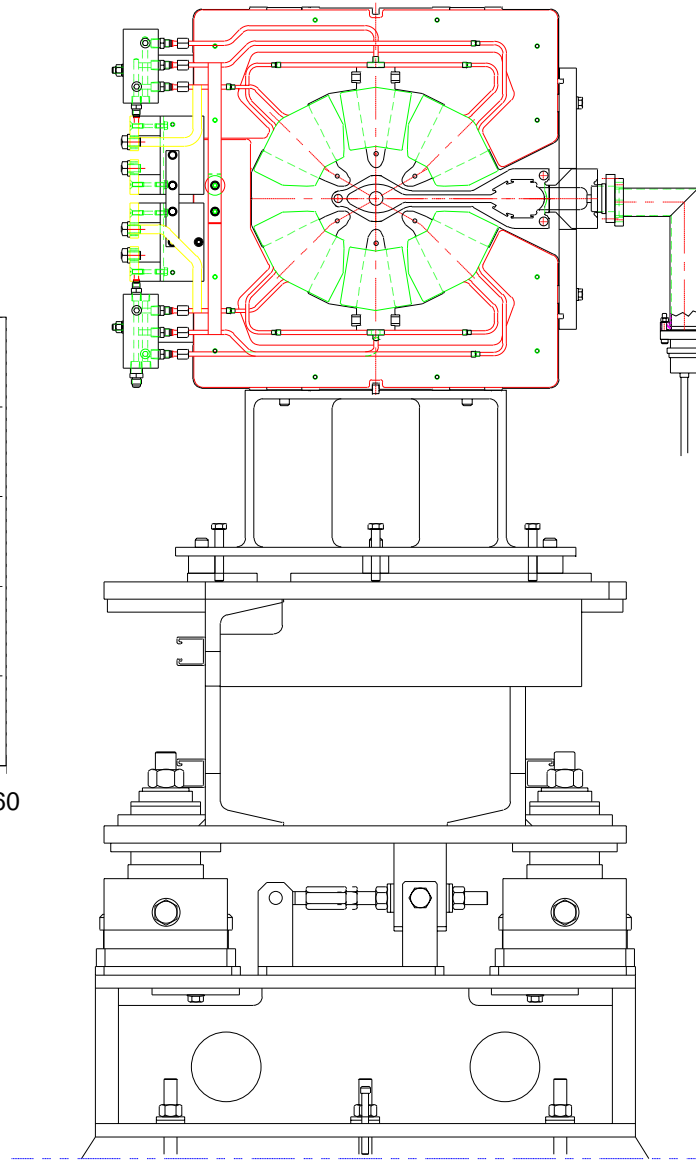
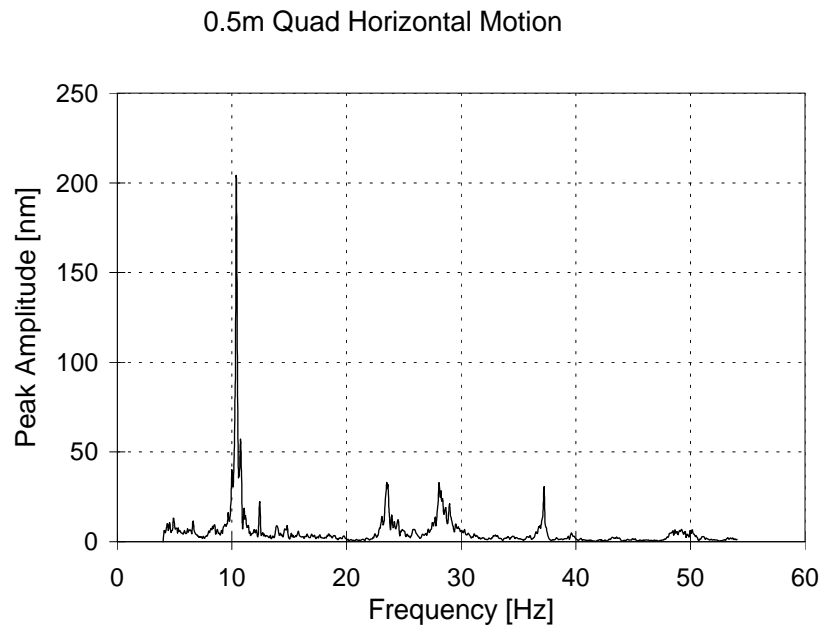
A Girder - End View



A Girder - Side View

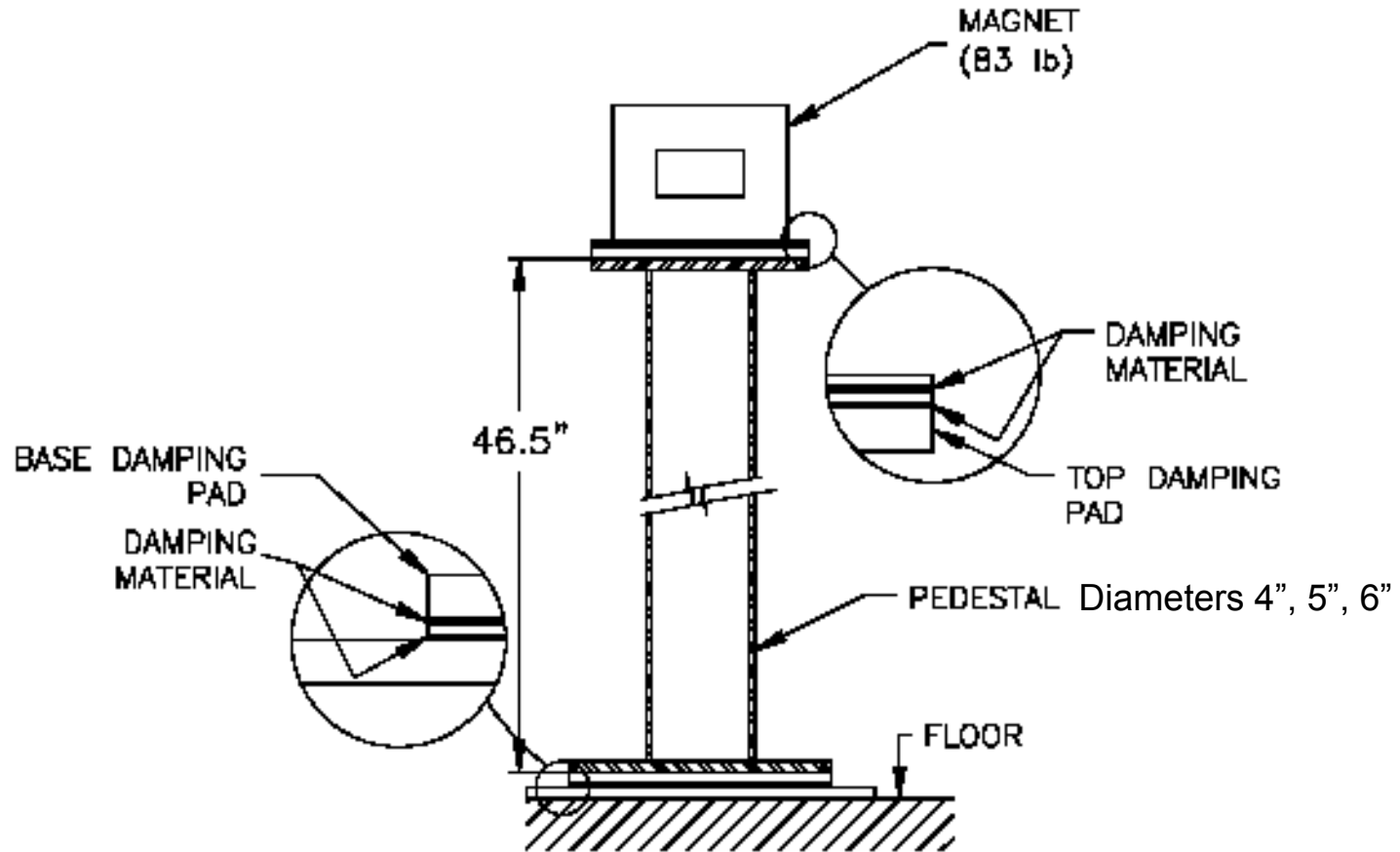


A Girder Resonance



G. Decker et al <http://accelconf.web.cern.ch/accelconf/p95/ARTICLES/FAR/FAR19.PDF>

Test Pedestal / Magnet Assembly

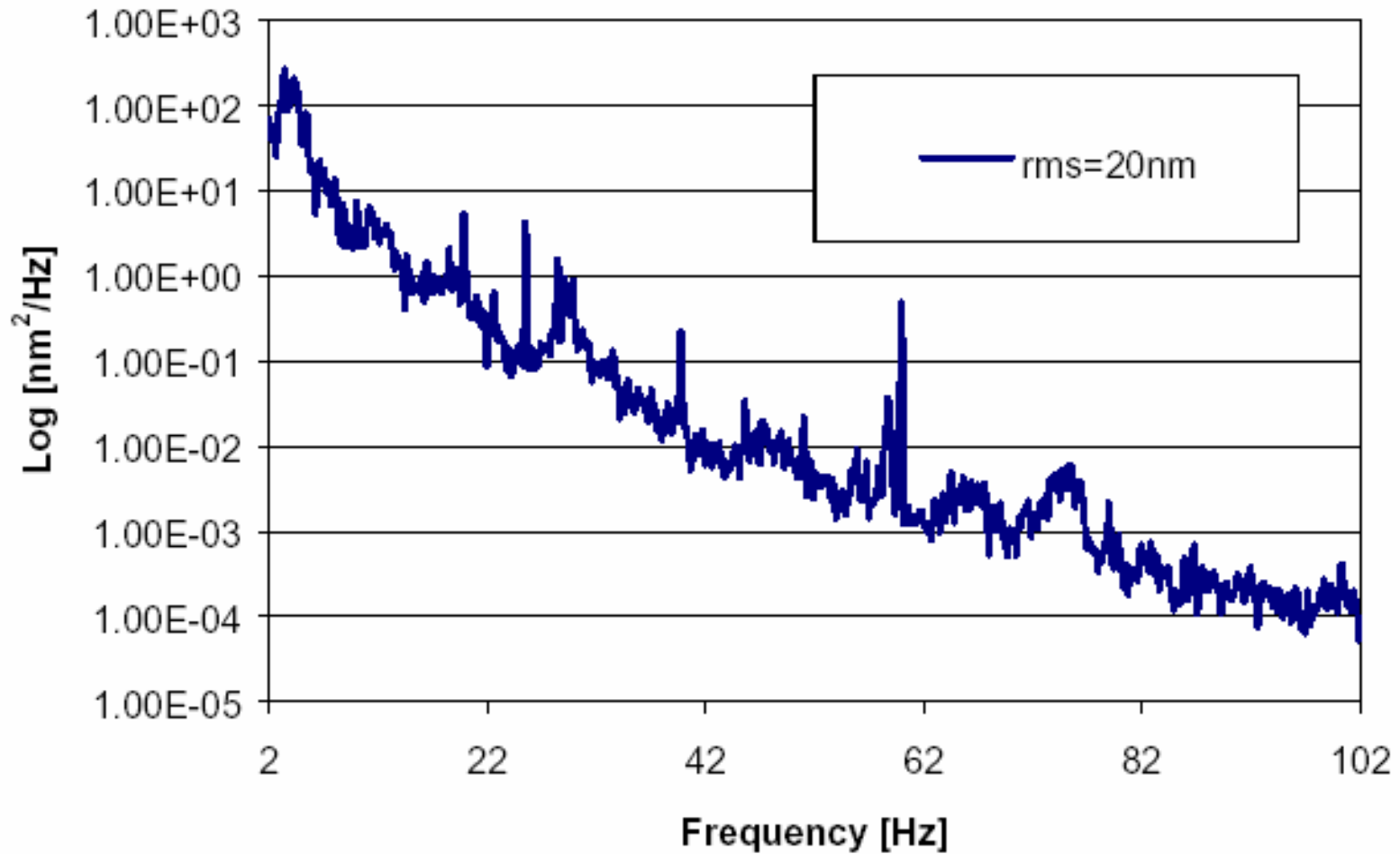


S. Sharma MEDSI 2000

[http://www.aps.anl.gov/asd/me/Public/Papers\(pdf\)/vibration.pdf](http://www.aps.anl.gov/asd/me/Public/Papers(pdf)/vibration.pdf)

Typical Ground Motion Spectrum

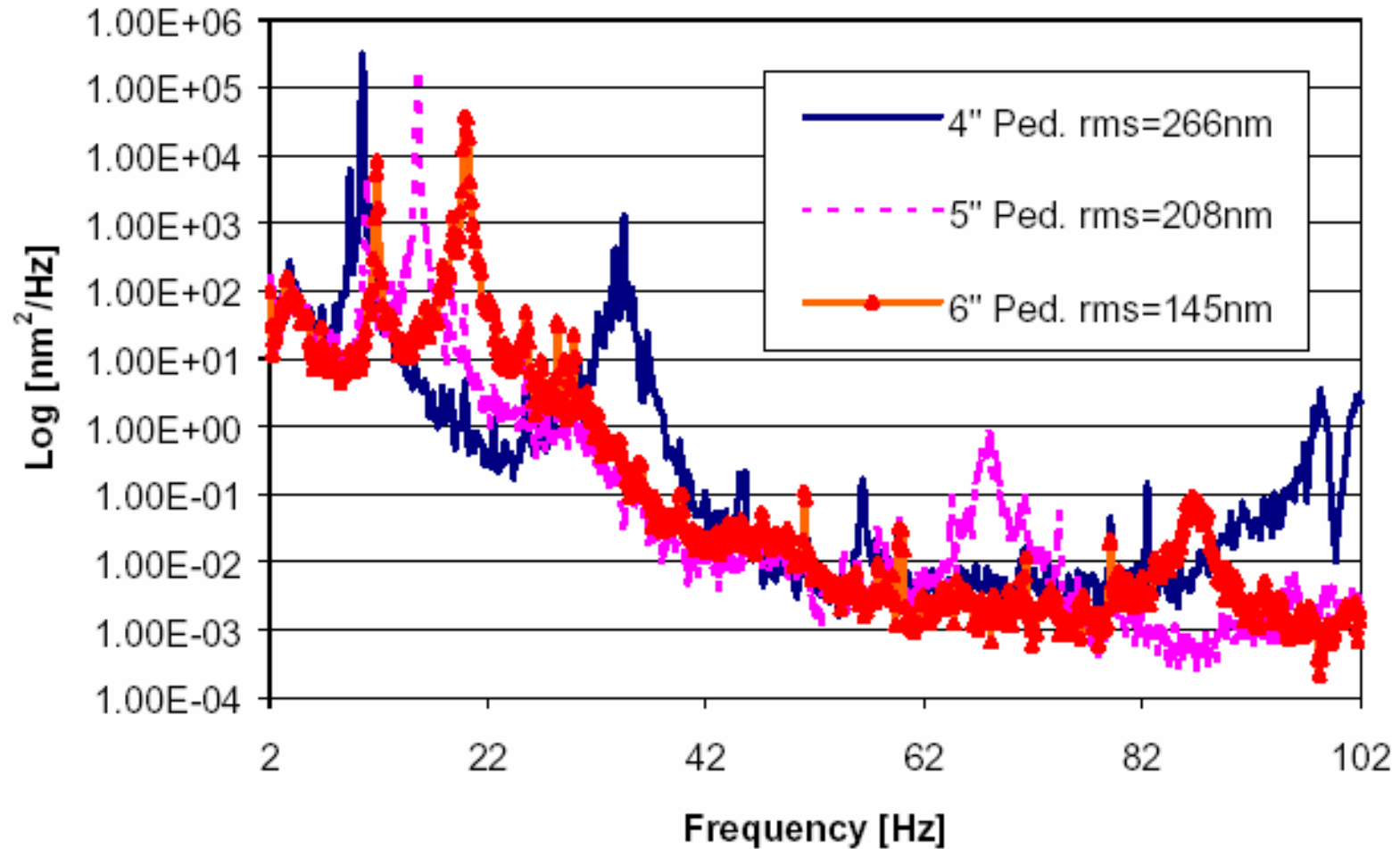
PSD of Ground Displacement



S. Sharma MEDSI 2000

[http://www.aps.anl.gov/asd/me/Public/Papers\(pdf\)/vibration.pdf](http://www.aps.anl.gov/asd/me/Public/Papers(pdf)/vibration.pdf)

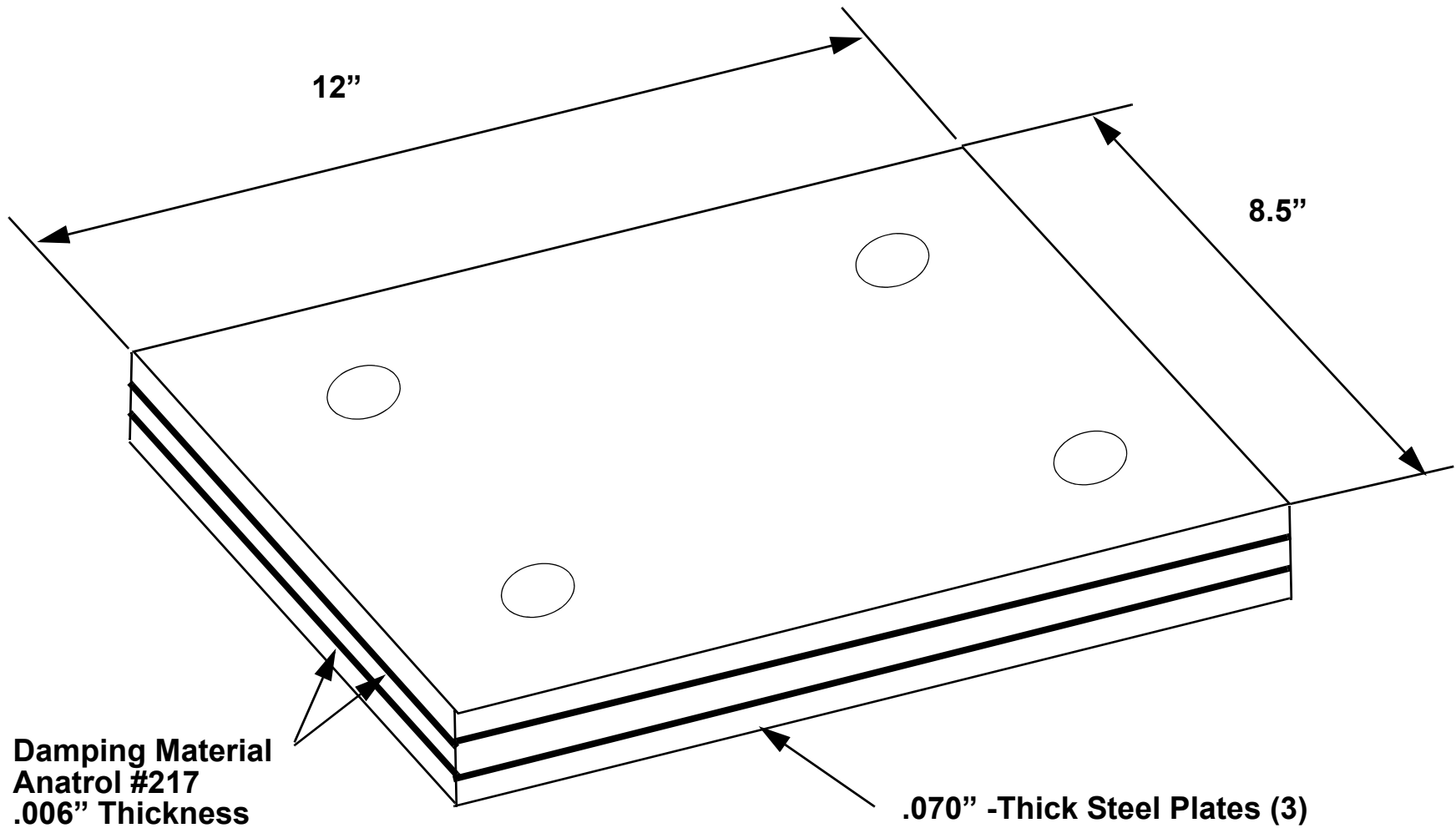
PSD of Magnet Displacement - No Damping



S. Sharma MEDSI 2000

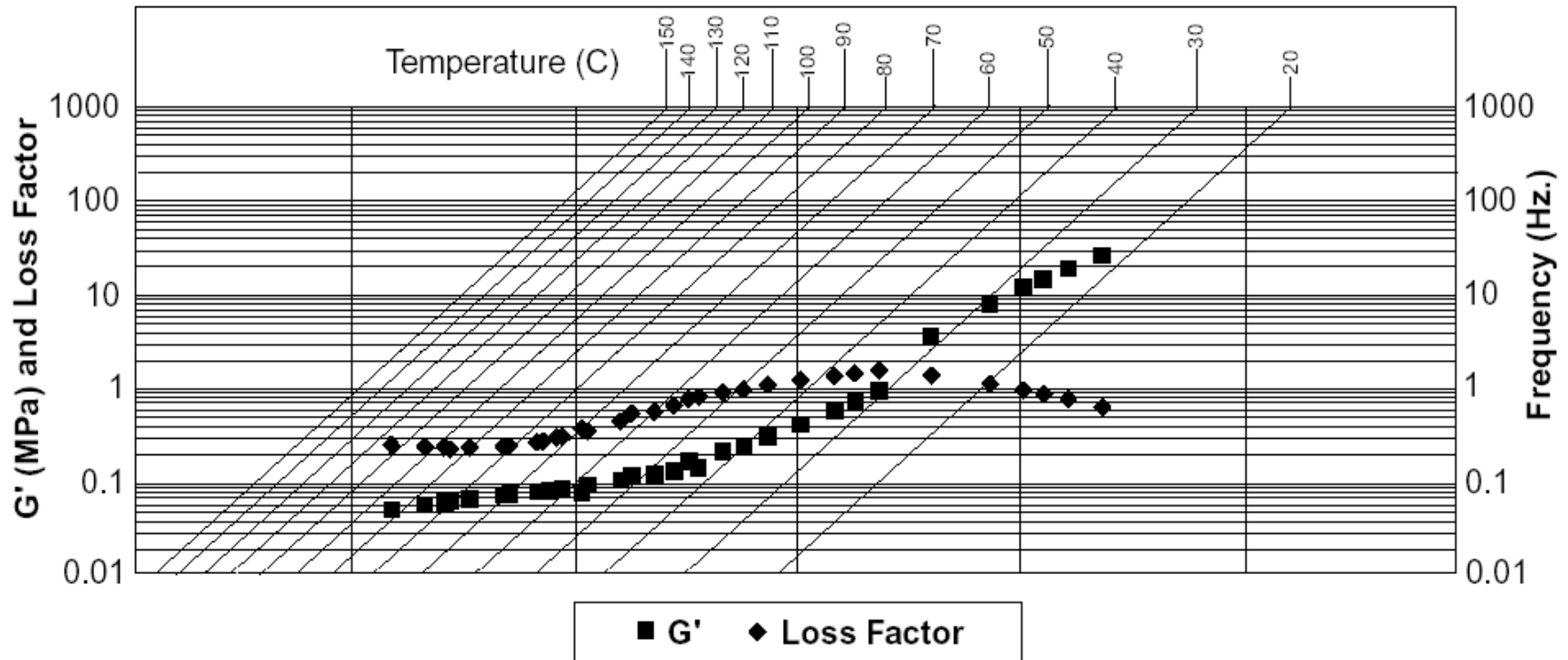
[http://www.aps.anl.gov/asd/me/Public/Papers\(pdf\)/vibration.pdf](http://www.aps.anl.gov/asd/me/Public/Papers(pdf)/vibration.pdf)

Laminated Damping Pad



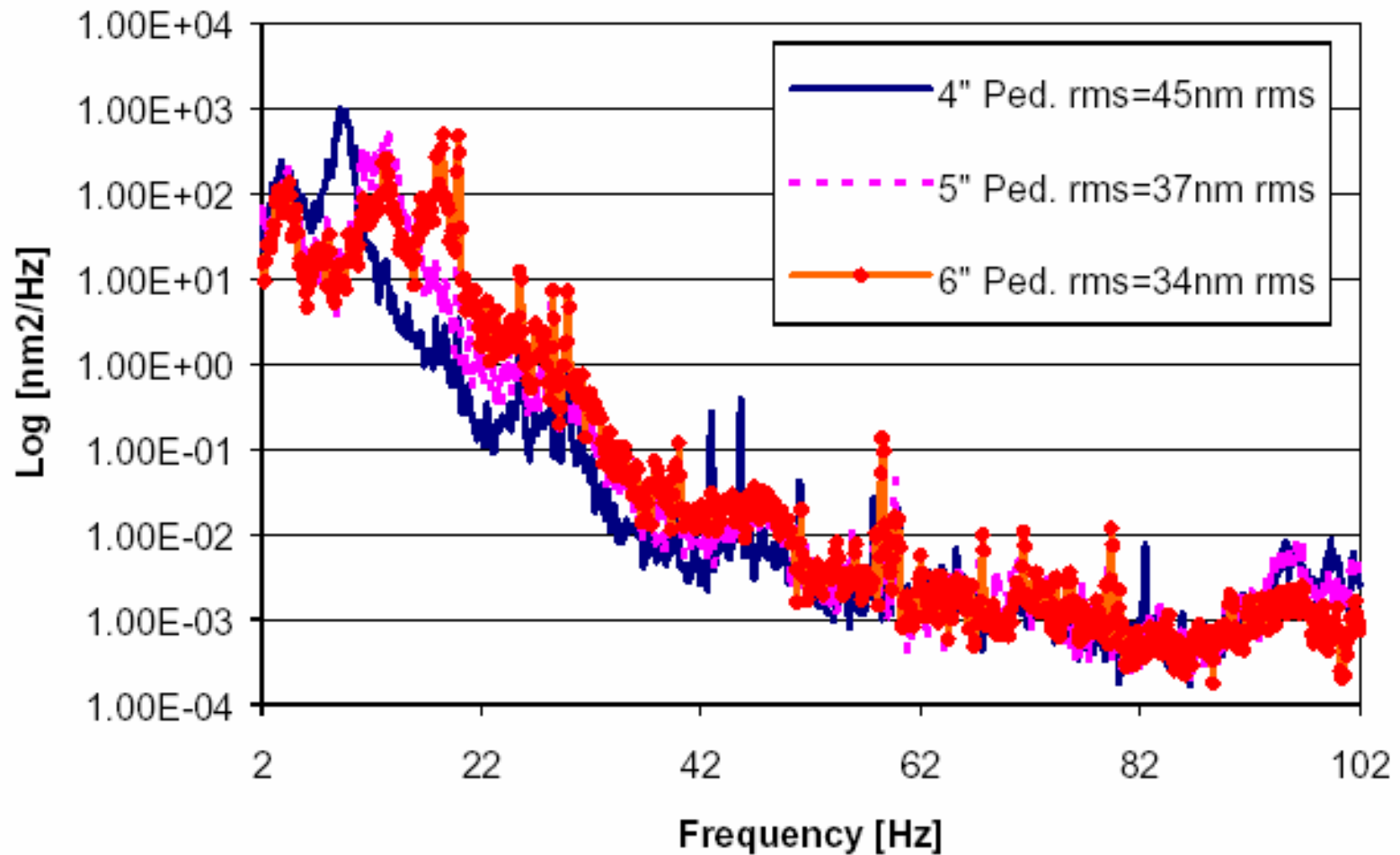
Visco-elastic Material Properties

3M™ Viscoelastic Damping Polymer 110 Nomograph

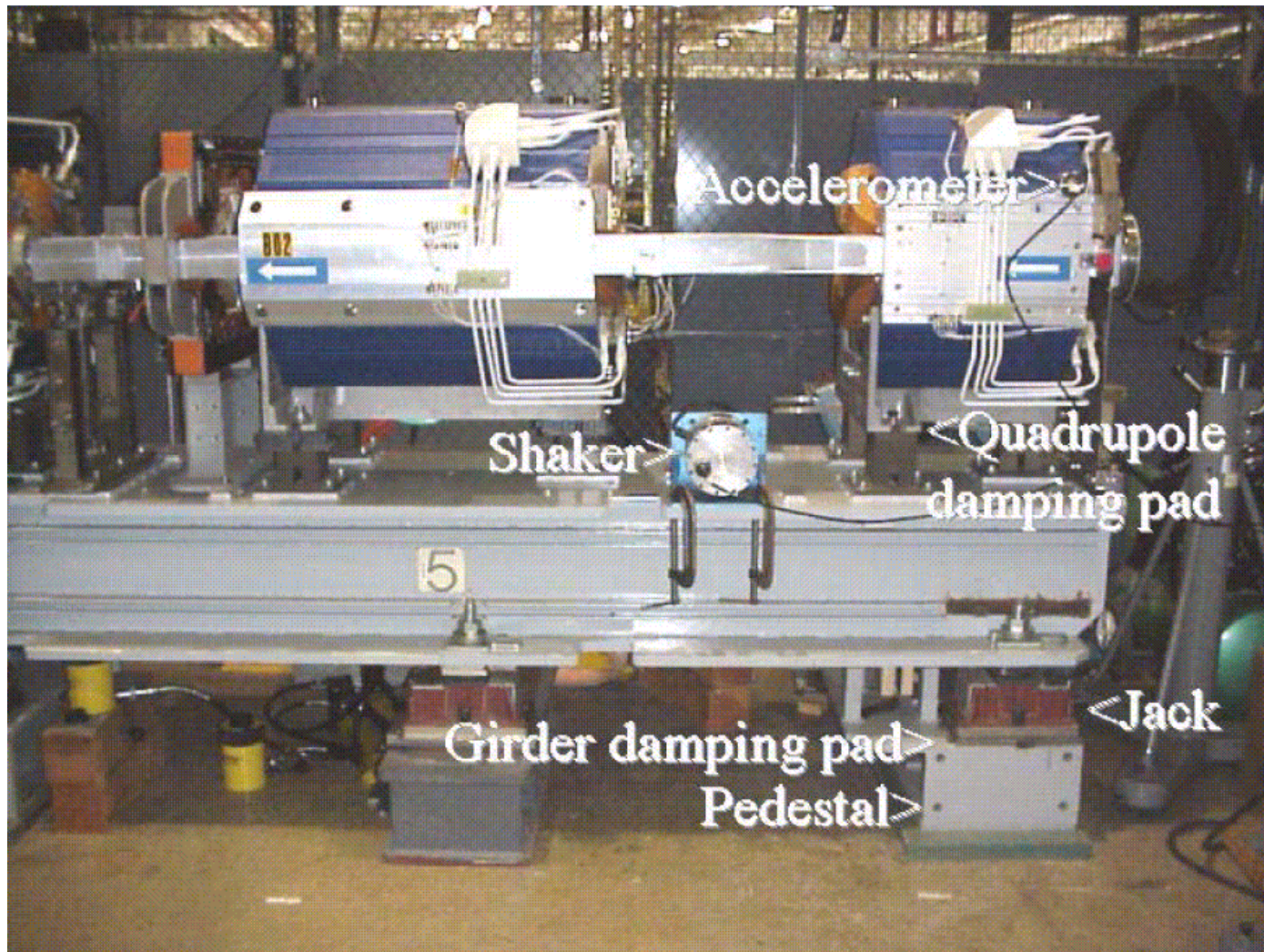


<http://multimedia.mmm.com/mws/mediawebserver.dyn?WWWWWWECOgjWpzXWizXWWWbEkGqUmxHb->

PSD of Magnet Displacement - Base and Top Damping

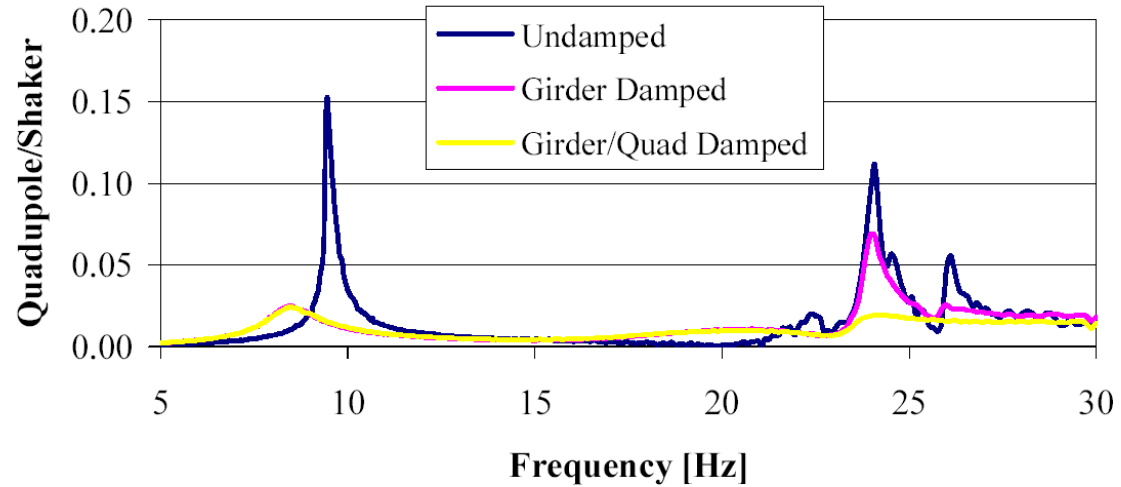


Girder Transfer Function Measurement Arrangement

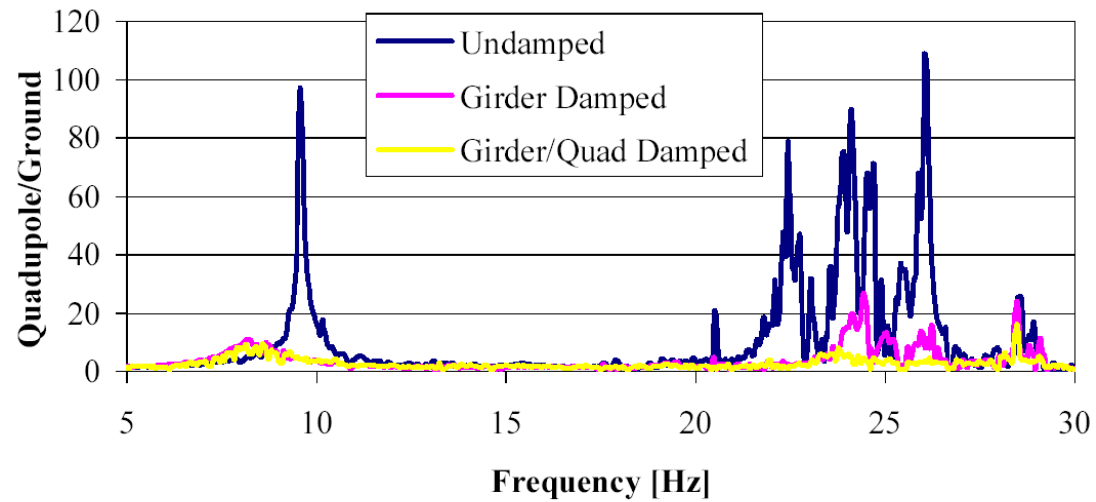


C. Doose, S. Sharma, MEDSI'02,
<http://www.aps.anl.gov/asd/me/medsi02/papers/MED021.pdf>

Case 1 Swept-Sine Measurement Transfer Functions

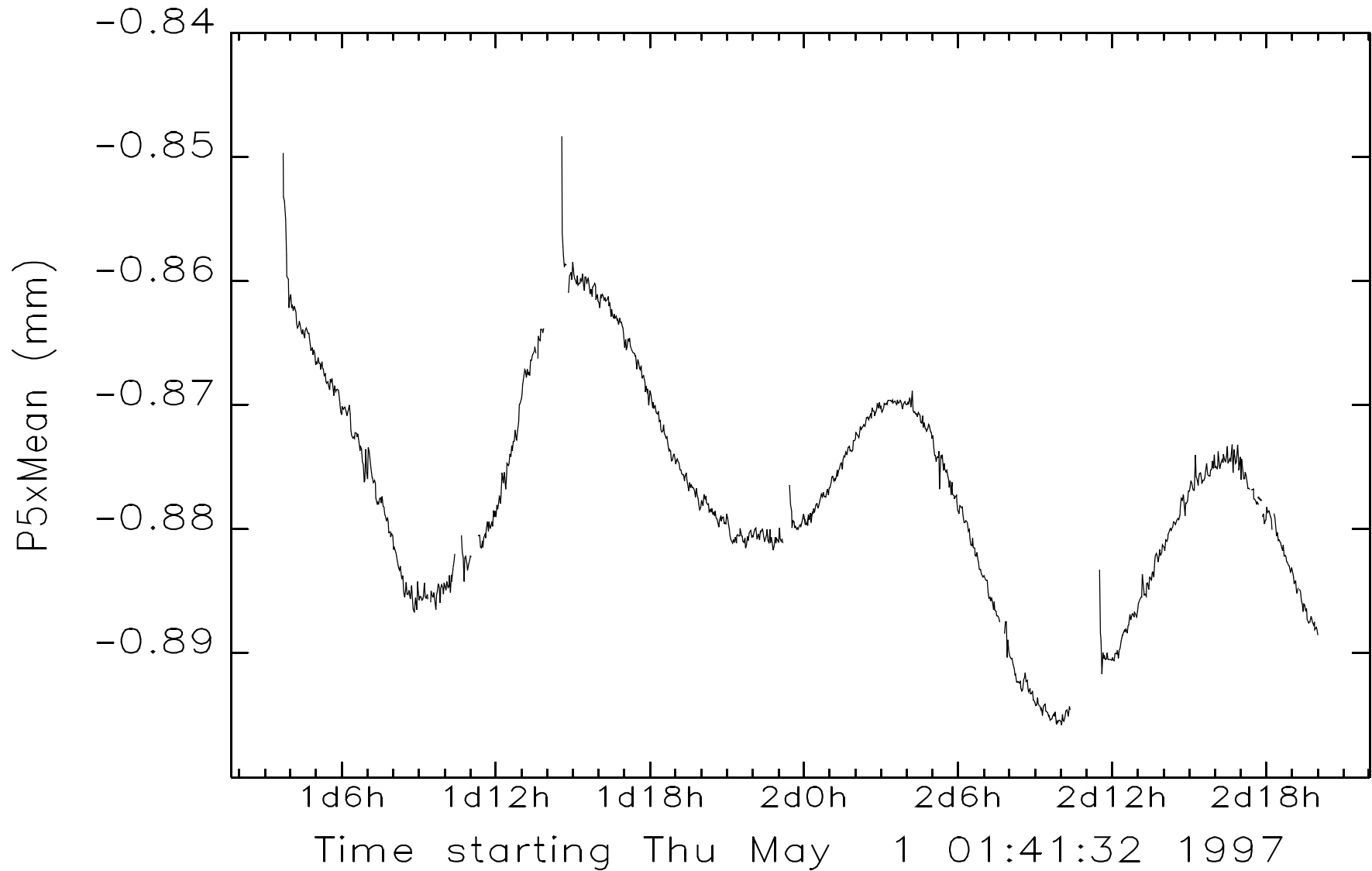


Case1 FFT Measurement Transfer Functions

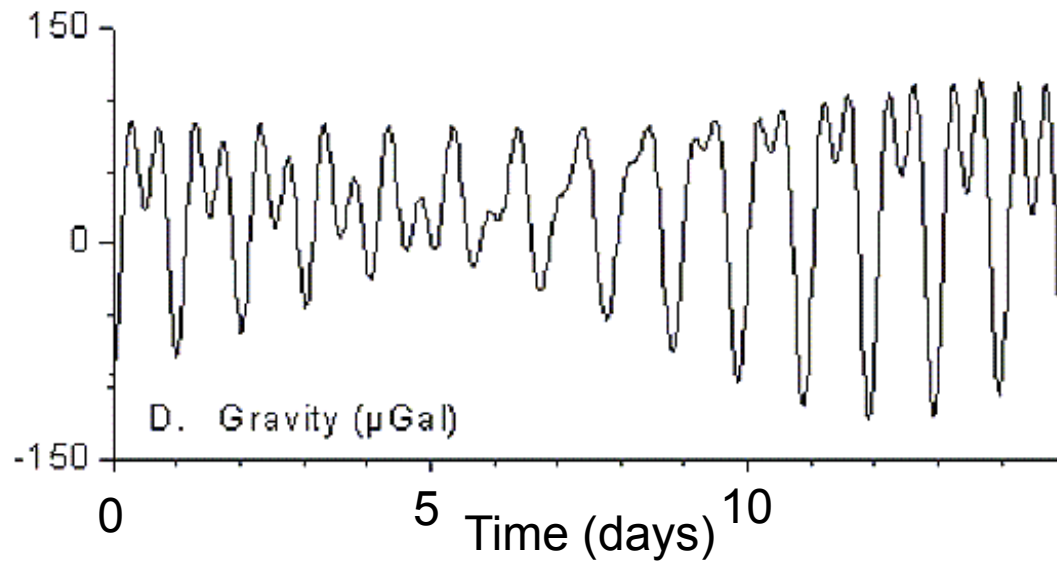


C. Doose, S. Sharma, MEDSI'02,
<http://www.aps.anl.gov/asd/me/medsi02/papers/MED021.pdf>

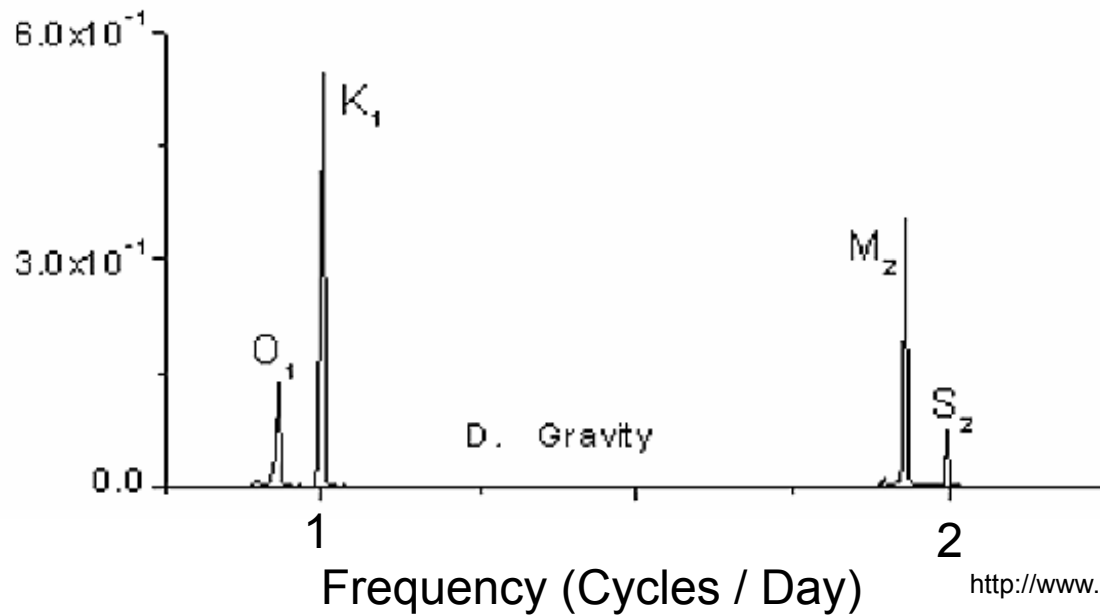
Horizontal Position Averaged at High Dispersion Locations



Gravity Fluctuations Showing Beating between Solar and Lunar Tides



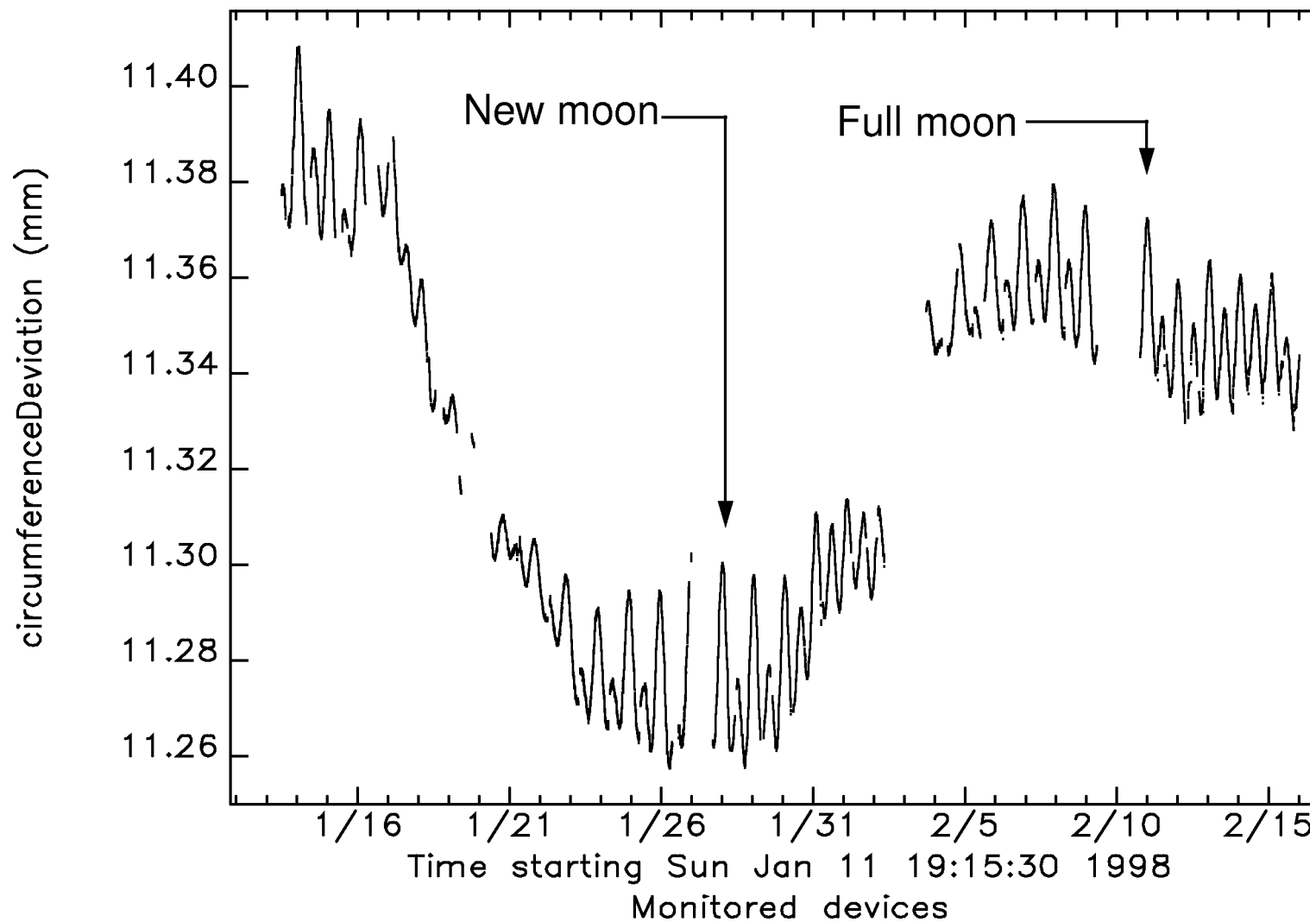
K₁, O₁, S₂, and M₂ respectively represent the luni-solar diurnal, principal lunar diurnal, principal solar semi-diurnal, and principal lunar semi-diurnal components.



Kulesa, B, et al, Geophys. Res. Lett., 30(1), 1011, (2003)

http://www.agu.org/pubs/sample_articles/cr/2002GL015303/5.shtml

Measured deviation of APS storage ring circumference from 1104 meter design value for operational period 98-1



Fourier transform of measured deviation of APS storage ring circumference
from 1104 meter design value for operational period 98-1

